Geosphere

Insights into southern Appalachian tectonics from ages of detrital monazite and zircon in modern alluvium

David Moecher, Jack Hietpas, Scott Samson and Suvankar Chakraborty

Geosphere 2011;7;494-512
doi: 10.1130/GES00615.1

Notes

THE GEOLOGICAL SOCIETY OF AMERICA

Insights into southern Appalachian tectonics from ages of detrital monazite and zircon in modern alluvium

David Moecher[1], Jack Hietpas[2], Scott Samson[2], and Suvankar Chakraborty[1]
[1]*University of Kentucky, Department of Earth and Environmental Sciences, Lexington, Kentucky 40517, USA*
[2]*Syracuse University, Department of Earth Sciences, Syracuse, New York 13244, USA*

ABSTRACT

Ages of detrital monazite and zircon from alluvium collected from the French Broad River drainage basin, an orogen-crossing main trunk river, and alluvium in first-order tributary streams, provide an unconventional perspective for examining the regional tectonic and metamorphic history of the southern Appalachian orogen (eastern United States). The French Broad River system samples migmatitic Ashe–Tallulah Falls suite paragneisses (with inferred Neoproterozoic clastic protoliths) of the Eastern Blue Ridge and western Inner Piedmont, Mesoproterozoic basement orthogneisses, numerous Paleozoic metaplutonic gneisses, and tectonite equivalents of these lithologies in the Brevard fault zone. Middle Ordovician ages dominate the monazite age spectrum. Monazite from tributaries has a dominant ^{208}Pb-^{232}Th age peak ca. 463 Ma. Monazite from the French Broad River alluvium suite yields a dominant ^{208}Pb-^{232}Th age mode ca. 450 Ma, but differs from the tributaries in having scattered Mesoproterozoic, Silurian–Devonian, and Carboniferous ages. Electron microprobe total Th-U-Pb chemical ages for selected tributary monazite grains also analyzed by ion microprobe reveal additional monazite growth events (i.e., metamorphic reaction) at 480–475 Ma and 445–440 Ma. Tributary and French Broad River zircon age spectra are dominated by Mesoproterozoic and Ordovician grains. Most Ordovician zircon from the French Broad River has Th/U > 0.1 and is most likely derived from the Henderson orthogneiss (447.6 ± 5.4 Ma), the largest pluton in the French Broad River headwaters region. A minor zircon age population at 450 Ma, represented primarily by metamorphic zircon rims with Th/U < 0.05 on magmatic Mesoproterozoic zircon cores, is present in tributaries and samples of migmatitic Ashe–Tallulah Falls suite paragneiss. Rare Neoproterozoic ages of 800–700 Ma and 600–550 Ma are present in all zircon data sets.

Ordovician monazite ages and zircon rim ages correspond to Taconian metamorphism in the Eastern Blue Ridge province. The dominant monazite age mode (463 Ma) from tributaries is slightly older than the Ordovician metamorphic zircon age mode (450 Ma), which is accounted for by monazite growth primarily via prograde metamorphic reactions, and zircon growth by melt-forming reactions in migmatites at the thermal peak. The scattered middle to late Paleozoic zircon and monazite ages attest to the lack of significant thermotectonic and magmatic events of that age in the Southern Blue Ridge providing sediment to the French Broad River drainage system. This dearth of ages is consistent with the pattern of nonpenetrative late Paleozoic deformation, retrograde metamorphism, and scattered plutonism northwest of the Brevard fault zone. A reasonable source of Neoproterozoic zircon in alluvium or in Ashe–Tallulah Falls paragneisses is Neoproterozoic rift-related magmatic rocks. The rarity of Mesoproterozoic monazite compared to zircon contrasts with the marked abundance of monazite in Ashe–Tallulah Falls paragneisses, and emphasizes the responsiveness of monazite compared to zircon in regional metamorphism. The abundant Mesoproterozoic zircon was inherited from Mesoproterozoic basement lithologies by Neoproterozoic sediments, preserved through regional metamorphism and three phases of orogenesis, and persists in modern alluvium being shed by the orogen.

INTRODUCTION

Direct dating of peak regional metamorphism accompanying collisional orogenesis ideally involves isotopic analysis of metamorphic minerals with high closure temperatures for diffusion of daughter isotopes. Use of metamorphic index minerals such as garnet, staurolite, and kyanite would be most definitive for claiming one is dating metamorphism (e.g., Lanzirotti and Hanson, 1995). However, the relatively low concentration of radiogenic parent isotopes (Sm, U) in these minerals and the prevalence of monazite or zircon inclusions (DeWolf et al., 1996) are limiting issues. Many geochronologic studies of regional metamorphic rocks have resorted to the use of monazite as a geochronometer (Parrish, 1990; Smith and Barreiro, 1990), as Th and U are major or minor elements in monazite, monazite contains very low initial Pb concentrations, and monazite growth can often be correlated with metamorphic reactions or fabric-forming deformation events attending porphyroblast growth (Foster et al., 2002; Williams and Jercinovic, 2002; Pyle and Spear, 2003; Gibson et al., 2004). Zircon is generally not amenable to dating low- and medium-grade regional metamorphism as its growth is usually limited to upper amphibolite to granulite facies conditions (Vavra et al., 1999; Rubatto et al., 2001). In addition to suitability for isotopic analysis, the growth history of monazite and zircon as revealed by microimaging methods can aid in interpreting the context of the metamorphic reaction and deformation history. This type of dating requires analytical methods with high spatial resolution, e.g., electron probe and ion probe microanalysis. Higher age precision may be attained using isotope dilution-thermal ionization mass spectrometry (ID-TIMS), but determination of metamorphic ages across a terrane requires a large number of samples, which is inefficient by ID-TIMS.

This study is an unconventional approach to dating regional metamorphism and contemporaneous magmatism that takes advantage of an extensive set of ages of detrital monazite and zircon separated from alluvium of the French Broad River, which drains an ~12,000 km^2 area of the southern Appalachian Blue Ridge. The samples were collected primarily for a comparison of the utility of detrital monazite versus detrital zircon ages as provenance indicators (Hietpas et al.,

Geosphere; April 2011; v. 7; no. 2; p. 494–512; doi: 10.1130/GES00615.1; 10 figures; 6 tables.

2010). Here we examine the monazite and zircon age distributions from this data set in more detail. Our study also incorporates new zircon secondary ion mass spectrometry (SIMS) U-Pb ages and monazite electron microprobe Th-U-Pb chemical ages for alluvium and bedrock samples collected in the context of zircon cathodoluminescence (CL) zoning, zircon Th/U values, and monazite compositional zoning, to determine the timing of regional metamorphic and magmatic events in the Blue Ridge and western Inner Piedmont. Although the original petrofabric and microstructural context of detrital monazite and zircon are unknown, we can tie the provenance of each grain to a probable source lithology based on its sample locality and in some cases on chemical characteristics (i.e., Th/U in zircon). The large number of grains analyzed in the Hietpas et al. (2010) study (1100 zircon analyses; 150 monazite analyses) combined with the wide sampling area and new SIMS and electron microprobe ages increases the likelihood of identifying less extensive metamorphic and magmatic events, and provides a terrane-scale context for those events.

GEOLOGIC SETTING

The broad outline of Blue Ridge tectonic history and distribution of regional metamorphic isograds have been known for decades (Hadley and Goldsmith, 1963; Carpenter, 1970; Butler, 1973; Rankin, 1975; Hatcher, 1978). However, the timing of metamorphic and magmatic events, based on high precision and high spatial resolution U-Pb geochronometers, has only recently been determined (Miller et al., 2000; Moecher et al., 2004a; Miller et al., 2006, 2010; Corrie and Kohn, 2007), and then only from scattered outcrops. There is also considerable ambiguity in the extent and intensity of each phase of metamorphism that has affected the southern Appalachians due to a series of overprinting Paleozoic collisional events.

The Blue Ridge in the southern Appalachians of western North Carolina is an amalgamation of Mesoproterozoic (Grenville age) basement rocks (mostly granitic orthogneisses), Neoproterozoic rift-related bimodal volcanic and plutonic rocks, late Neoproterozoic to Early Ordovician rift and passive margin, mostly clastic sedimentary cover sequences (Ocoee Supergroup, Ashe Metamorphic Suite, Chilhowee Group), and Ordovician plutonic rocks (Fig. 1A). These Blue Ridge components were first metamorphosed together in the Middle Ordovician. Regional metamorphism reached upper amphibolite facies with extensive development of migmatites in pelitic and mafic bulk compositions. Granulite facies assemblages in pelitic and mafic bulk compositions occur locally (Absher and McSween, 1985; Eckert et al., 1989), as well as the most extensive tract of eclogite facies rocks in the Appalachian orogen (Willard and Adams, 1994; Miller et al., 2010). Middle to late Paleozoic metamorphism is greenschist (in basement, eastern and western Blue Ridge cover sequences) to amphibolite facies (Blue Ridge thrust complex, western Inner Piedmont) and not penetratively developed, compared to early Paleozoic metamorphism and compared to the extent of Acadian metamorphism in the northern Appalachians. Plutons of early, middle, and late Paleozoic age in the Blue Ridge, emplaced into a compressional setting, were variably deformed by each phase of orogenesis.

Uncertainty regarding the setting for early and middle Paleozoic tectonism and plutonism is largely the result of late Paleozoic collision and formation of crystalline thrust sheets that transported the complex of Precambrian and Paleozoic units westward onto the Laurentian margin (Hatcher, 1987). Greenschist facies mylonite zones define thrust sheet boundaries and occur throughout Blue Ridge basement as 1–10-km-wide anastomosing zones of Mississippian age mylonites (Merschat et al., 2006). Late Paleozoic deformation also resulted in folding at all observable scales and retrograde metamorphism of early Paleozoic assemblages (Massey and Moecher, 2005; Clemons and Moecher, 2009).

The French Broad River headwater streams collect alluvium from both sides of the northeastern-striking Brevard fault zone (Fig. 1B). The Eastern Blue Ridge in the French Broad headwaters includes the Mesoproterozoic Toxaway Gneiss (Carrigan et al., 2003), Neoproterozoic metasediments of the Ashe–Tallulah Falls suite (ATFS, Hatcher, 2002; Bream et al., 2004), the Ordovician Whiteside pluton, and Devonian Looking Glass and Pink Beds plutons (Miller et al., 2000). The southeast side of the Brevard zone includes the western Inner Piedmont, dominantly mica schists, migmatitic gneisses, and amphibolites of the ATFS. From its headwaters near Rosman (North Carolina), the French Broad River flows northeast parallel to the Brevard fault zone, turns north through Asheville and across the migmatitic pelitic gneisses and amphibolites of the ATFS (Rankin et al., 1973; McSween et al., 1989; Hatcher, 2002), then turns northwestward across mostly Blue Ridge basement rocks to the Great Smoky fault (base of the crystalline thrust sheets) in western North Carolina and eastern Tennessee (Fig. 1B). The main tributary of the French Broad is the Pigeon River, which cuts across the eastern end of the Great Smoky Mountains and has local headwater tributaries in the Canton quadrangle (Fig. 1B). Metamorphism in the study area ranges from sillimanite grade in the southeast to chlorite grade in the northwest (Carpenter, 1970; Hadley and Nelson, 1971).

Mesoproterozoic (ca. 1350–900 Ma) basement rocks are dominantly upper amphibolite facies, migmatitic layered gneisses enclosing 1–10-km-scale masses of weakly foliated granulite facies orthogneisses. The granulite assemblages are demonstrably Mesoproterozoic (Carrigan et al., 2003; Ownby et al., 2004), whereas the migmatitic layered gneisses are probably the product of upper amphibolite facies early Paleozoic metamorphism of rocks with Mesoproterozoic protoliths (Merschat et al., 2006). The ATFS in the study area is dominantly migmatitic metapelitic gneisses with conspicuous leucosomes and a mineral assemblage of plagioclase + biotite + kyanite/sillimanite + garnet + quartz + rutile + muscovite (Fig. 2). Minor components of the ATFS include amphibolites and calc-silicates. Trondhjemite dikes and pegmatites of Silurian to Devonian age are volumetrically minor but widespread in the area west and north of Asheville, and could potentially contribute detrital zircon to modern alluvium. The kyanite-sillimanite isograd bisects the Canton quadrangle (Merschat and Wiener, 1988).

Known regional tectonometamorphic and magmatic events in the drainage basin of the French Broad and Pigeon Rivers include Mesoproterozoic magmatism and granulite facies metamorphism, Neoproterozoic continental rift magmatism (Goldberg et al., 1986; Su et al., 1994; Aleinikoff et al., 1995; Tollo et al., 2004) (and potential contact or hydrothermal metamorphism), and Paleozoic plutonism and regional metamorphism. The early Paleozoic Henderson orthogneiss is one of the largest Paleozoic plutons in the Southern Blue Ridge, and is bedrock along much of the upper course of the French Broad River (Fig. 1B).

Based on U-Pb zircon and monazite geochronology from localities elsewhere in the Blue Ridge of western North Carolina, peak Paleozoic amphibolite, granulite, and eclogite facies metamorphism is Middle Ordovician in age (Moecher et al., 2004a, 2005; Corrie and Kohn, 2007; Miller et al., 2010). Hornblende ^{40}Ar-^{39}Ar plateau ages in the study area range from 410 to 450 Ma (Dallmeyer, 1975; Kunk et al., 2006), but variably disturbed hornblende isotopic systematics are widespread (Goldberg and Dallmeyer, 1997). The Rb-Sr and Sm-Nd mineral-rock isochrons from samples in the vicinity of the Lick Ridge eclogite support the interpretation of Middle Ordovician regional metamorphism with variable Devonian resetting (Goldberg and Dallmeyer, 1997). Muscovite

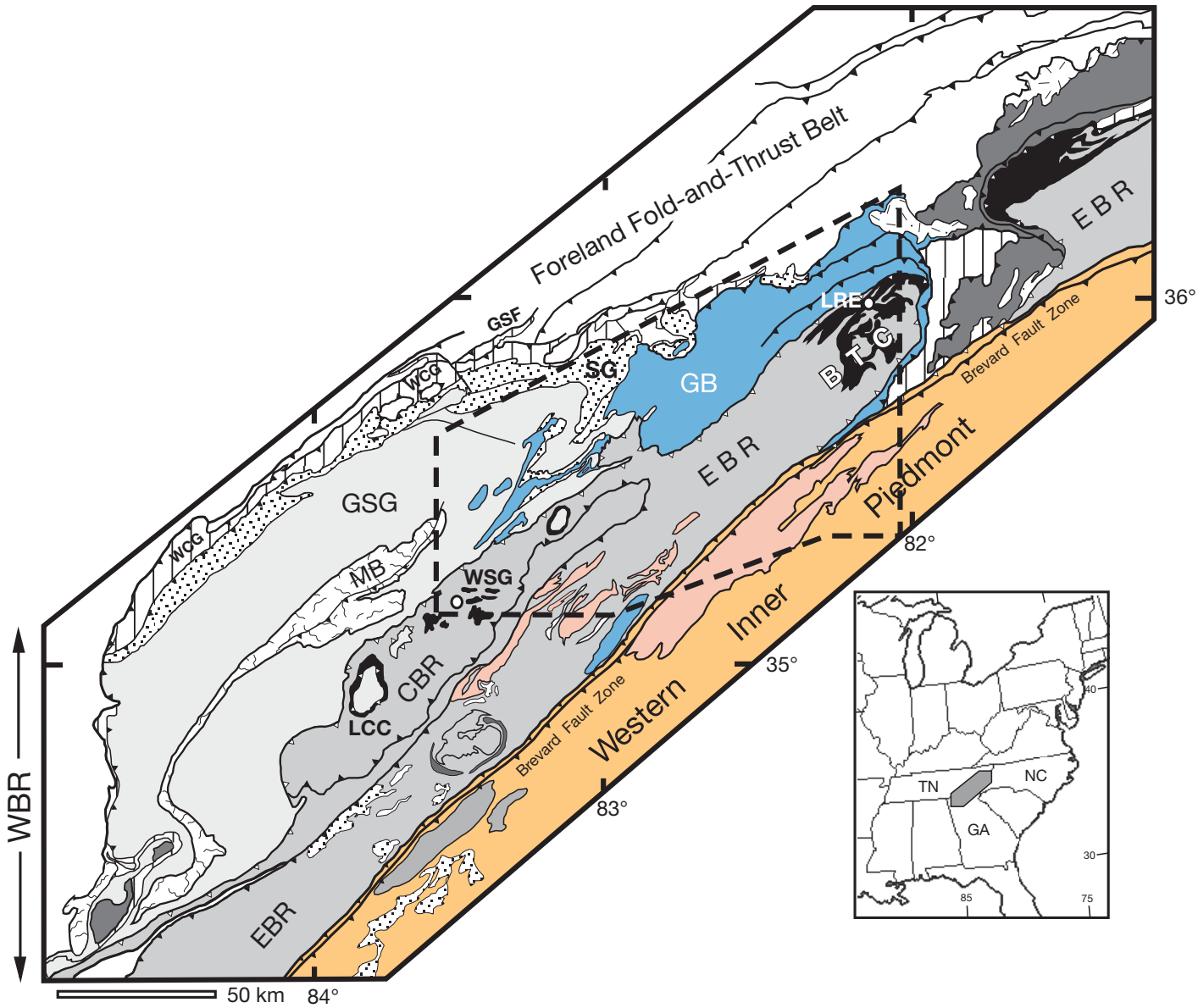

Figure 1 (*on this and following page*). (A) Generalized geologic map of the southern Appalachian orogen (after Rankin et al., 1990). Dashed outline is approximate study area, shown in Figure 1B. BTC—Blue Ridge thrust complex; CBR—Central Blue Ridge; EBR—Eastern Blue Ridge; GB—Grenville basement; GSF—Great Smoky fault; GSG—Great Smoky Group; LCC—Lake Chatuge mafic complex; LRE—Lick Ridge eclogite; MB—Murphy Belt; SG—Snowbird Group; WBR—Western Blue Ridge; WCG—Walden Creek Group; WSG—Winding Stair Gap.

^{40}Ar-^{39}Ar plateau and Rb-Sr mineral-rock isochron ages throughout the entire study area are generally Carboniferous (Dallmeyer, 1988; Connelly and Dallmeyer, 1993; Goldberg and Dallmeyer, 1997; Kunk et al., 2006).

METHODS

For our earlier study (Hietpas et al., 2010) samples of coarse sand were collected from the French Broad River at 14 sites extending from its headwaters near Rosman, North Carolina, to Douglas Lake near Newport, Tennessee (Fig. 1B). An additional sample was collected from the Pigeon River near its confluence with the French Broad River. Heavy mineral concentrates in alluvium from tributary streams in the Canton quadrangle (Fig. 1B; Table 1) were originally obtained from the North Carolina Geological Survey (Merschat and Wiener, 1988) and made available for the Hietpas et al. (2010) study. The tributary stream samples were collected in the context of 1:24,000 scale bedrock mapping and must be derived from either ATFS schist and migmatitic paragneiss (Fig. 2, A-1–A-3) or Mesoproterozoic Sandymush and Earlies Gap gneisses (Merschat and Cattanach, 2008) (Table 2), as these are the only lithologic units observed in the quadrangle (Merschat and Wiener, 1988). The western half of the Canton quadrangle drains into downstream stretches of the French Broad River via the Pigeon River, and the eastern half drains directly into the French Broad River.

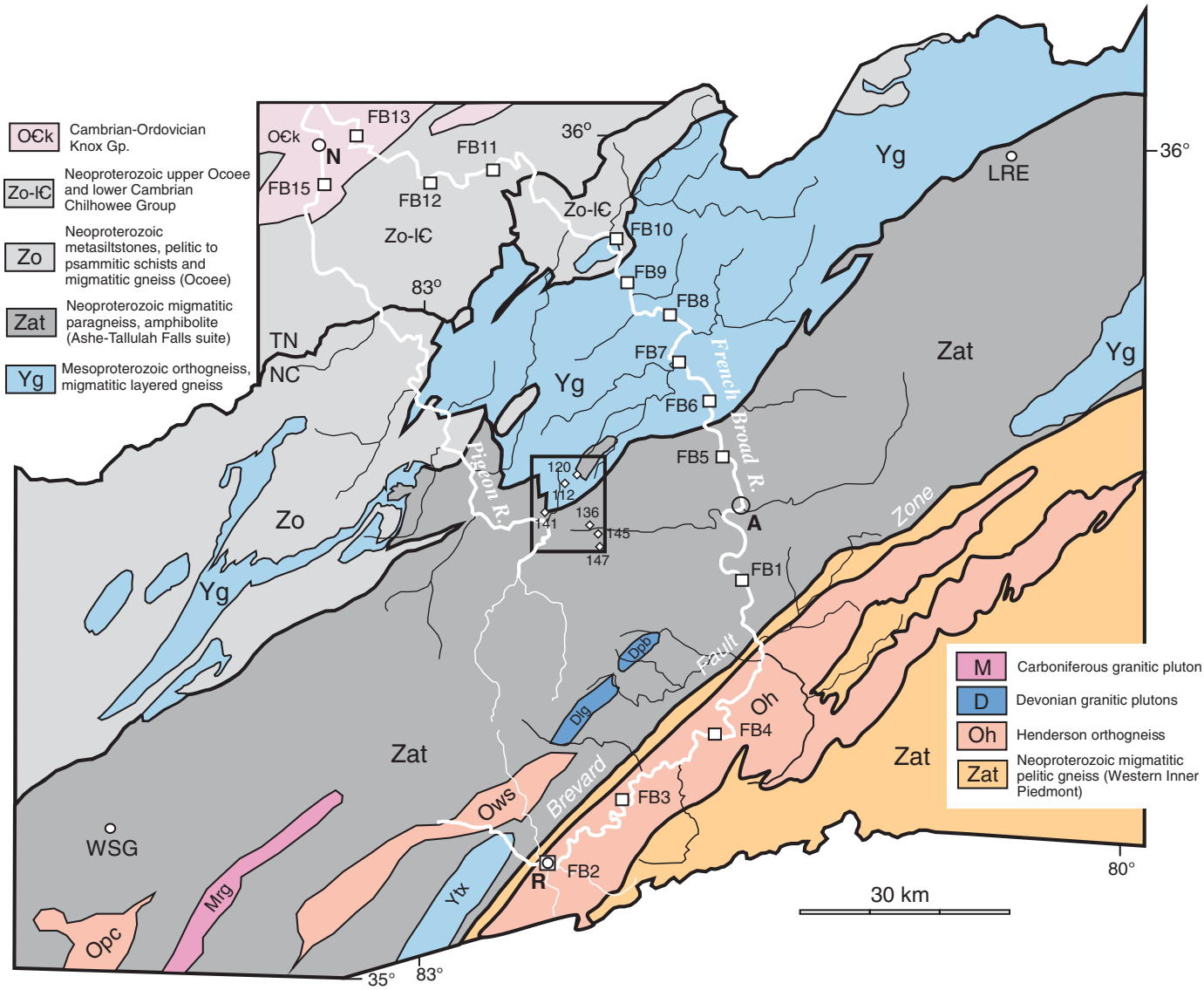

Figure 1 (*continued*). (B) Geologic map of western North Carolina delineating ages of potential detrital sediment source terranes in French Broad–Pigeon River drainage systems, showing alluvium sample locations (FB1–13 and FB15) and location of first-order tributary stream samples (CT prefix in data tables and figs.) in Canton quadrangle (black box). Dlg—Looking Glass granite; Dpb—Pink Beds granite; LRE—Lick Ridge eclogite locality; Mrg—Rabun granite; Oh—Henderson orthogneiss; Opc—Persimmon Creek gneiss; Ows—Whiteside granite; WSG—Winding Stair Gap roadcut; A—Asheville; R—Rosman, North Carolina; N—Newport, Tennessee.

Additionally for this study, fresh samples of migmatitic Ashe paragneiss, Ashe pelitic schist, and Henderson orthogneiss were collected from roadcuts near tributary and alluvium sample sites. The rock samples were crushed and processed using heavy liquids and magnetic separation to concentrate zircon for ion microprobe dating.

Monazite and zircon in river and stream alluvium, and crushed rock samples, were handpicked from all recognizable populations based on size, crystal morphology, and color. Other random approaches for mounting grains for analysis (e.g., pouring grains from a vial) result in a bias for larger grains. Zircon from Mesoproterozoic orthogneisses is generally much larger and more abundant than zircon from Paleozoic Appalachian granitic plutons (Moecher and Samson, 2006). Therefore, any approach for mounting grains that might introduce a size bias would also bias the age distributions. Zircon or monazite crystals, along with age standards, were embedded in epoxy. Cured mounts were then ground to expose the interiors of the crystals. Each monazite crystal was imaged before ion probe analysis by backscattered electron imaging using the JEOL 8600 Superprobe at Syracuse University. Representative monazite grains analyzed by ion microprobe were also selected for electron microprobe wavelength dispersive X-ray elemental mapping to determine the nature and extent of growth zoning, which was used to guide monazite electron probe microanalysis. Every zircon analyzed in this study was imaged using cathodoluminescence to determine relative proportion of cores and rims as a guide for microanalysis, to assess magmatic versus metamorphic growth (Hanchar and Miller, 1993; Corfu et al., 2003),

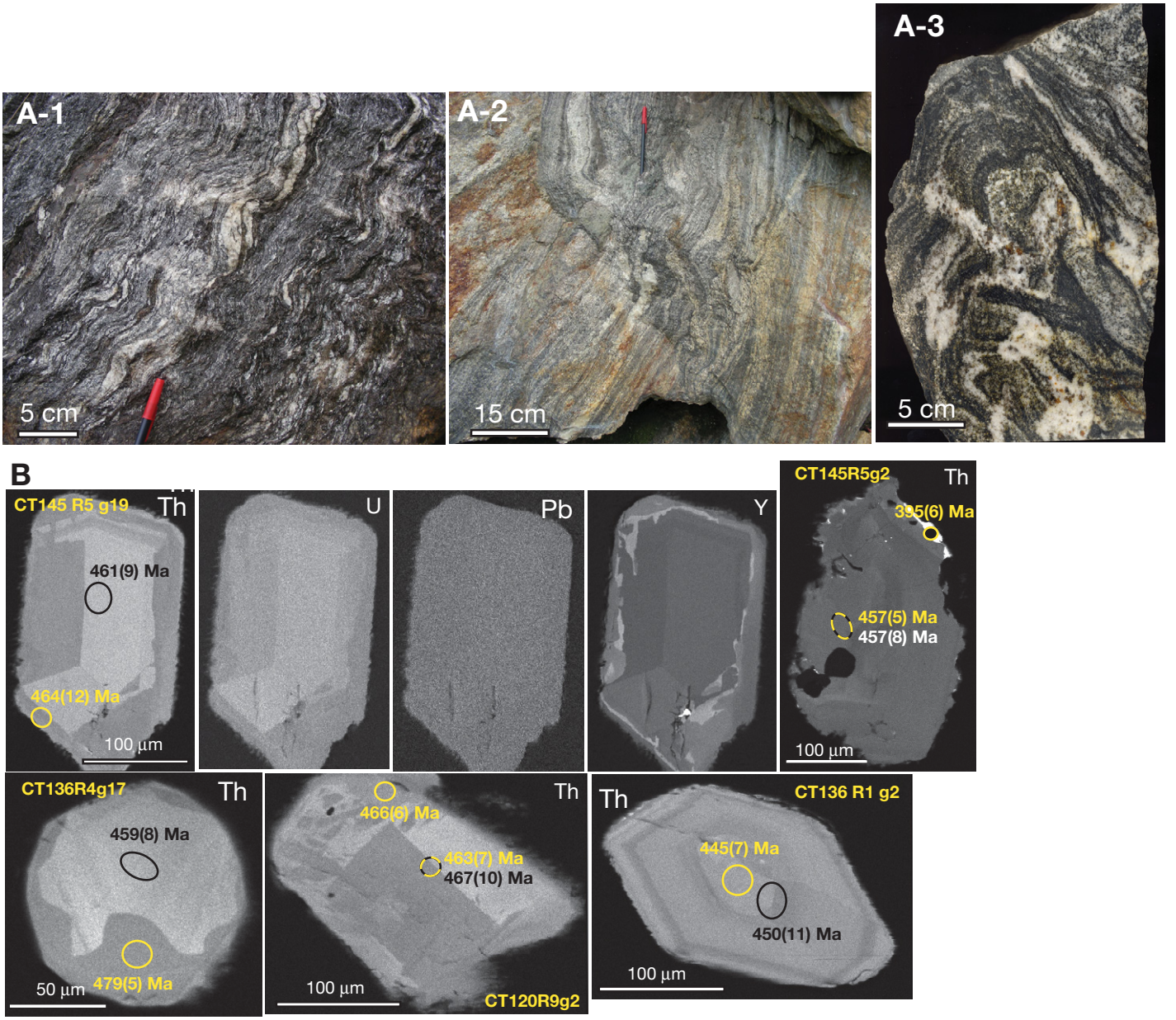

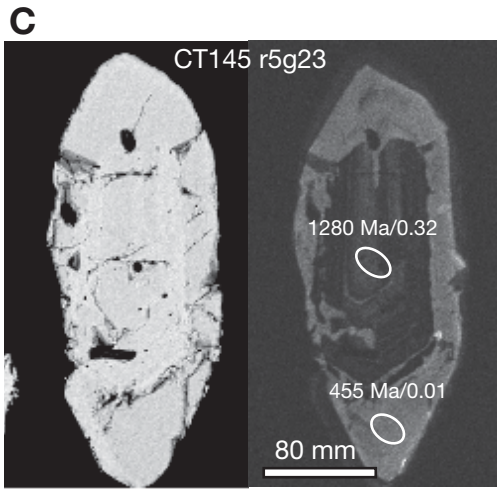

Figure 2. Images of representative rocks and minerals analyzed in this study, and ages determined by ion and electron probe microanalysis (EPMA) (ion probe data from Hietpas et al., 2010). (A-1, A-2) Biotite-rich and felsic migmatitic gneisses, respectively, of Ashe–Tallulah Falls series that crop out in Canton quadrangle, North Carolina (location in Fig. 1B). (A-3) Slab of ATFS (Ashe–Tallulah Falls suite) migmatite from Canton quadrangle showing leucosomes and late folds. (B) Wavelength dispersive elemental X-ray maps for monazite dated by ^{208}Pb-^{232}Th ion probe microanalysis and Th-U-Pb EPMA (age errors given in parentheses). All maps for relevant elements shown for one sample, with Th maps shown for other monazites. Locations of electron beam (yellow circles; 5–6 microprobe analyses are made within the area of the circle) or ion probe beam (black; dashed where spots overlap), with respective ages (yellow—electron microprobe; black—ion microprobe), are shown for each grain. (C) Representative backscattered electron (BSE; left) and cathodoluminescence (CL; right) images of zircon from Canton quadrangle stream sample CT145 sourced mainly in ATFS migmatitic gneiss, showing age and Th/U for each zone. Zoned magmatic Grenville core is overgrown by light gray unzoned Taconian metamorphic rim with very faint (dark gray; compare shape of grain in BSE and CL images) thin outer rim that is too narrow for ion probe analysis. EPMA ages are compiled in Table 3.

TABLE 1. MODAL ANALYSES OF PANNED HEAVY MINERAL CONCENTRATES, CANTON QUADRANGLE, NORTH CAROLINA

Sample	Lithology	Zone	Mag (%)	Ilm (%)	Hbl (%)	Epid (%)	Grt (%)	Staur (%)	Ky (%)	Sil (%)	Monaz (%)	Titan (%)	Rut (%)	Zrc (%)	Tour (%)
CT112	Ye, Zas	Sil	29.5	17.5	1.0	2.0	21.5	1.0	3.5	1.0	3.5	0	0.5	19.0	0
CT120	Ye, Zas	Sil	6.0	18.5	9.0	4.5	30.5	tr	8.5	4.0	12.5	0	1.0	5.5	0
CT136	Zag	Sil	11.0	28.0	0	0	34.5	1.0	1.5	2.5	8.0	0	0.5	13.0	0
CT141	Ye, Zas	Ky	4.5	53.5	0	0	2.5	0.5	27.5	0	4.5	0.5	0.5	6.0	0
CT145	Zag	Sil	9.0	26.5	1.0	0	21.0	13.5	12.0	1.0	7.0	0	2.0	7.0	0
CT147	Zag	Sil	13.5	24.0	0.5	0	27.5	5.5	1.0	1.0	9.0	2.5	0	15.5	0

Note: Data Source: Merschat and Wiener (1988). Ye—Earlies Gap gneiss; Zas—ATFS (Ashe–Tallulah Falls suite) schist; Zag—ATFS gneiss; tr—trace; Sil—sillimanite; Mag—magnetite; Ilm—ilmenite; Hbl—hornblende; Epid—epidote; Grt—garnet; Staur—staurolite; Ky—kyanite; Monaz—monazite; Titan—titanite; Rut—rutile; Zrc—zircon; Tour—tourmaline.

and to ensure that analytical spots did not overlap core-rim boundaries. In most cases the cores of monazite and zircon were analyzed, and rims of zircon were analyzed if of sufficient width to accommodate the laser beam.

Monazite ^{208}Pb/^{232}Th was measured using SIMS on the CAMECA 1270 at the University of California Los Angeles as described in Hietpas et al. (2010) (also see Harrison et al., 1995). The ^{208}Pb-^{232}Th system was used because Th is a major element in monazite, leading to higher signal intensities and shorter analysis times, an important factor when high throughputs are necessary for assembling a detrital age data set.

Some detrital zircon U-Pb ages were also determined by SIMS using the CAMECA 1270 instrument at the University of California Los Angeles (Grove et al., 2003). One important advantage of SIMS analysis is that only a few nanograms of zircon are consumed in the analysis and that no mineralogical or chemical change occurs in the crystal being analyzed. Thus the technique can be viewed as nondestructive. The majority of the detrital zircon crystals, however, were dated using laser ablation–multicollector–inductively coupled plasma mass spectrometry (LA-MC-ICP-MS) techniques on the Isoprobe-P at the LaserChron Center of the University of Arizona (Gehrels et al., 2008). As with SIMS analysis, LA-ICP-MS ages are dependent on comparison of ages of natural zircon standards. The main differences between techniques are that the LA-ICP-MS dating technique is much faster than SIMS (~1 min compared to ~15 min), but the former uses considerably more material (at least hundreds of nanograms) and physically alters the zircon by preferentially extracting uranium compared to Pb from the analyzed region (Patchett and Samson, 2004). Thus this technique must be viewed as at least partially destructive. The analytical data and calculated ages for accessory minerals from modern alluvium are available in Hietpas et al. (2010). Accessory mineral ages for potential source rocks are presented here.

Selected monazites from the tributary streams draining areas underlain by Ashe paragneisses that were analyzed by SIMS for ^{208}Pb-^{232}Th geochronology were also analyzed by electron probe microanalysis (EPMA) for total Th-U-Pb chemical age determinations (Montel et al., 1996; Pyle et al., 2005; Williams et al., 2007). This method measures the total Pb concentration in monazite and assumes that all Pb is radiogenic, produced by decay of ^{235}U, ^{238}U, and ^{232}Th. Monazite typically contains higher concentrations of Th than U (usually 1–5 wt% ThO_2, 0.1–1 wt% UO_2; Montel et al., 1996), so that most of the radiogenic Pb results from Th decay. Total Pb concentrations range from 100 to 1000 ppm, which can be measured precisely via EPMA with high beam currents, long count times, and careful background measurements (Williams et al., 2006). The amount of nonradiogenic Pb in monazite is sufficiently low (1–3 ppm; Parrish, 1990; Hawkins and Bowring, 1997) as to not significantly affect the calculated chemical age of monazite. The greatest limitation of the chemical age method is that discordance of the U-Pb system cannot be assessed. The advantage of EPMA chemical age dating is that the electron microprobe has one to two orders of magnitude higher spatial resolution than the ion microprobe, allowing for analysis of multiple and smaller growth generations in a single monazite grain than with the ion microprobe.

Monazite EPMA for this study was carried out at the University of Massachusetts on the CAMECA Ultrachron microprobe following the analytical protocol of Williams et al. (2006) and Williams and Jercinovic (2002). Semi-quantitative X-ray maps of monazite grains

TABLE 2. ION MICROPROBE AGES FOR MONAZITE FROM CANTON TRIBUTARY STREAMS

Sample No. **Canton quad.**	^{208}Pb-^{232}Th age (Ma)	Error (Ma)	Sample No. **Canton quad.**	^{208}Pb-^{232}Th age (Ma)	Error (Ma)
ct136r1g1	547	11	ct141r12g9	451	10
ct136r1g2	450	11	ct141r12g10	466	12
ct136r1g4	461	8	ct112R14G22	461	10
ct136r1g5	465	10	ct 112R14G23	465	9
ct136r1g7	461	10	ct 112R14G24	477	9
ct136r1g8	454	10	ct 112R14G25	483	9
ct136r1g11	459	9	ct 112R14G28	472	10
ct136r1g12	461	9	ct145r6g22	470	10
ct135r1g11	459	9	ct145r6g21	476	11
ct136r1g14	455	9	ct145r6g20	471	9
ct136r1g15	474	9	ct145r6g19	466	10
ct136r1g16	467	8	ct145r6g17	466	9
ct136r1g17	459	8	ct145r5g17	466	10
ct112r13g26	476	10	ct145r5g18	465	10
ct112r13g25	474	9	ct145r5g19	461	9
ct112r13g24	470	8	ct145r5g21	472	8
ct112r13g23	473	8	ct145r5g16	461	9
ct112r13g22	470	10	ct145r5g9	460	10
ct112r13g1	458	9	ct145r5g10	438	9
ct112r13g2	458	11	ct145r5g11	460	9
ct112r13g3	464	11	ct145r5g12	467	8
ct112r13g4	465	9	ct145r5g13	463	10
ct112r13g5	460	9	ct145r5g1	455	10
ct120r9g1	460	9	ct145r5g2	457	8
ct120r9g2	467	10	ct145r5g3	453	10
ct120r9g3	462	7	ct145r5g5	459	9
ct120r9g4	458	9	ct145r7g1	453	10
ct120r9g6	463	8	ct145r7g2	455	8
ct141r12g3	449	9	ct145r7g3	456	9
ct141r12g6	465	9	ct145r7g5	453	9
ct141r12g7	455	11	ct145r7g6	462	8

Note: Data from Hietpas et al. (2010).

were used to determine growth domains based on the distribution of Th, U, and Y, followed by complete EPMA quantitative analysis of 6–8 points in each zone. Measured Th, U, and Pb contents (with Y correction) are used to calculate a date for each point (Table 3). Age precision for each point is based on X-ray counting statistics. Individual point analyses (5–10) are pooled to calculate a weighted mean age and error for a generation of monazite growth that is interpreted to be geologically meaningful (time of growth of that zone, representing a phase of mineral reaction; Foster et al., 2002; Spear and Pyle, 2002; Williams and Jercinovic, 2002; Wing et al., 2003; Gibson et al., 2004; Williams et al., 2007; Corrie and Kohn, 2008).

RESULTS

Monazite

Monazite grains from the Canton quadrangle tributaries exhibit Th, U, and Y compositional zoning patterns consisting of sector zoned cores that compose the bulk of the grain with thin rims overgrowing embayed margins (Fig. 2B). The ^{208}Pb-^{232}Th ages are Ordovician (Fig. 3A; Table 2). All but three ages are within analytical error [generally ±5–10 m.y. (1σ) for monazite ^{232}Th-^{208}Pb ages] in the range 455–475 Ma. The age distribution is slightly skewed to younger ages and the distribution appears to consist of two age populations if plotted with 5 m.y. bins (Fig. 4A).

Monazite grains from French Broad River alluvium are dominated by Middle Ordovician ages, but yield a greater range of Ordovician ages than those of the Canton quadrangle tributary streams, and include scattered Mesoproterozoic ages, three Neoproterozoic ages, and numerous middle to late Paleozoic ages (Fig. 4). The Ordovician age mode consists of a major peak at 455–460 Ma and a spread of ages from 455 to 425 Ma (Fig. 4C). The French Broad samples also have minor populations of Devonian and Carboniferous ages, which are absent in the tributary alluvium. The majority of the younger ages are from samples FB1 to FB4, which were collected southeast of the Brevard fault zone, but could be derived from streams in the French Broad headwaters region that collect alluvium from either side of the fault zone (Fig. 1B). Sample FB15 (Fig. 1B; Table 2), collected in the floodplain of the Pigeon River, yields an age range similar to the French Broad River and tributary streams.

Electron microprobe total Th-U-Pb chemical ages of detrital monazite from Canton quadrangle tributaries are dominantly Middle Ordovician, with rare Cambrian, Silurian, and Devonian ages (Table 3). Three grains for which the same growth zone was analyzed by both EPMA and ion probe yield identical ages (467 ± 10 versus 463 ± 7; 461 ± 9 versus 464 ± 12; 457 ± 8 versus 457 ± 5 Ma; Fig. 2; Table 3). For other monazite grains, distinctive growth zones as defined by differences in Th or U concentration, may yield the same total Th-U-Pb chemical age, or they may yield analytically different ages, and rims may be older than cores, which is not uncommon in monazite due to resorption and embayment followed by overgrowth by new monazite (Spear and Pyle, 2002). The chemical age of 479 ± 5 Ma (sample CT136, Table 3) is similar to the oldest monazite ion probe ages for tributary samples (475–485 Ma). However, the youngest chemical age (395 ± 5 Ma) is for a narrow Th-rich rim zone that is too thin to analyze precisely by ion probe and younger than the youngest ion probe age for the tributaries (Fig. 2B). Although this Devonian age is not detected by ion probe, similar middle Paleozoic ages occur in upper French Broad River alluvium samples (see following).

Zircon

Zircon from Canton tributary samples (Tables 4 and 6) has oscillatory zoned cores with Th/U values consistent with magmatic crystallization, and unzoned rims and Th/U consistent with metamorphic growth (Fig. 2C). Dominant age peaks occur at 1190, 1050, and 450 Ma, with minor peaks at 1290 and 1800 Ma (Fig. 5A). No ages younger than ca. 420 Ma were found. The Canton tributary samples are dominated by Mesoproterozoic zircon with age distributions that are identical to French Broad alluvium samples collected in areas draining Mesoproterozoic basement northwest of Asheville (e.g., FB6–FB10, Fig. 1B). Neoproterozoic ages are rare in Canton quadrangle stream samples. Values of Th/U for zircon with Ordovician ages are 0.01–0.06, which contrasts with Th/U values in Mesoproterozoic zircon from the tributaries of 0.11–2.25 (Fig. 5D). Neoproterozoic zircon, although rarer, has Th/U of 0.06–0.41. Rock samples of ATFS migmatitic gneiss and schist exhibit an age distribution similar to those of tributary streams (Table 5; Fig. 5E), with fewer Ordovician zircons and rare Neoproterozoic ages. The former have very low Th/U (0.01–0.03) (Fig. 5F; Table 5).

The dominant zircon age population in French Broad alluvium samples is Middle Ordovician (ca. 450 Ma) (Fig. 6A); secondary populations occur at 1150–1190 and 1000–1050 Ma, similar to tributary zircon age distributions. Neoproterozoic ages are much less abundant than Mesoproterozoic ages, but span the entire eon (Fig. 7A). The Ordovician zircons exhibit a range of Th/U (Fig. 8B), indicating that a mix of metamorphic and magmatic zircon defines that population. The dominant age population in French Broad alluvium is the same as the age of zircon from rock samples of the Henderson orthogneiss, which has relatively high Th/U (0.45–1.14; Table 5) and yields a concordia age of 447.6 ± 5.4 Ma (Fig. 9; Table 5). Zircon in Ashe paragneiss and schist is dominantly Mesoproterozoic, with scattered Neoproterozoic ages, and a distinct Ordovician peak (Fig. 5E; Table 5). The Ordovician zircon has distinctly lower Th/U values than the Mesoproterozoic and Neoproterozoic zircon in the Ashe bedrock samples (Fig. 5F), which are similar to values for zircon in tributary samples (Fig. 5D).

TABLE 3. MONAZITE TH-U-PB ELECTRON PROBE MICROANALYSIS CHEMICAL AGES, BEDROCK SAMPLES OF ASHE GNEISS

	Age (Ma) Spot No.								EPMA		SIMS	
Sample No.	1	2	3	4	5	6	7	8	Ave (Ma)	Error (Ma)	Age (Ma)	Error (Ma)
CT136 r1g2 hiU core	442	441	435	451	451	450			445	7	450	11
CT136 r4 g17 rim	476	480	480	484	478	472	474	488	479	5	459	8
CT120 r9 g2 core	452	463	466	458	468	473			463	7	467	10
CT120 r9 g2 rim	456	465	465	476	464	468			466	6		
CT145 r5 g19 up rim	455	478	468	453					464	12	461	9
CT145 r5 g2 core	458	465	452	453	455	456			457	5	457	8
CT145 r5 g2 hiTh rim	388	391	400	393	398	402			395	6		
CT147 r8 g8 outer rim	428	432	433	431	420	418	452		427*	6		
CT147 r8 g8 hiY core	504	492	508	505	502	513	520	523	504	10		

*Average age excludes spot 7.

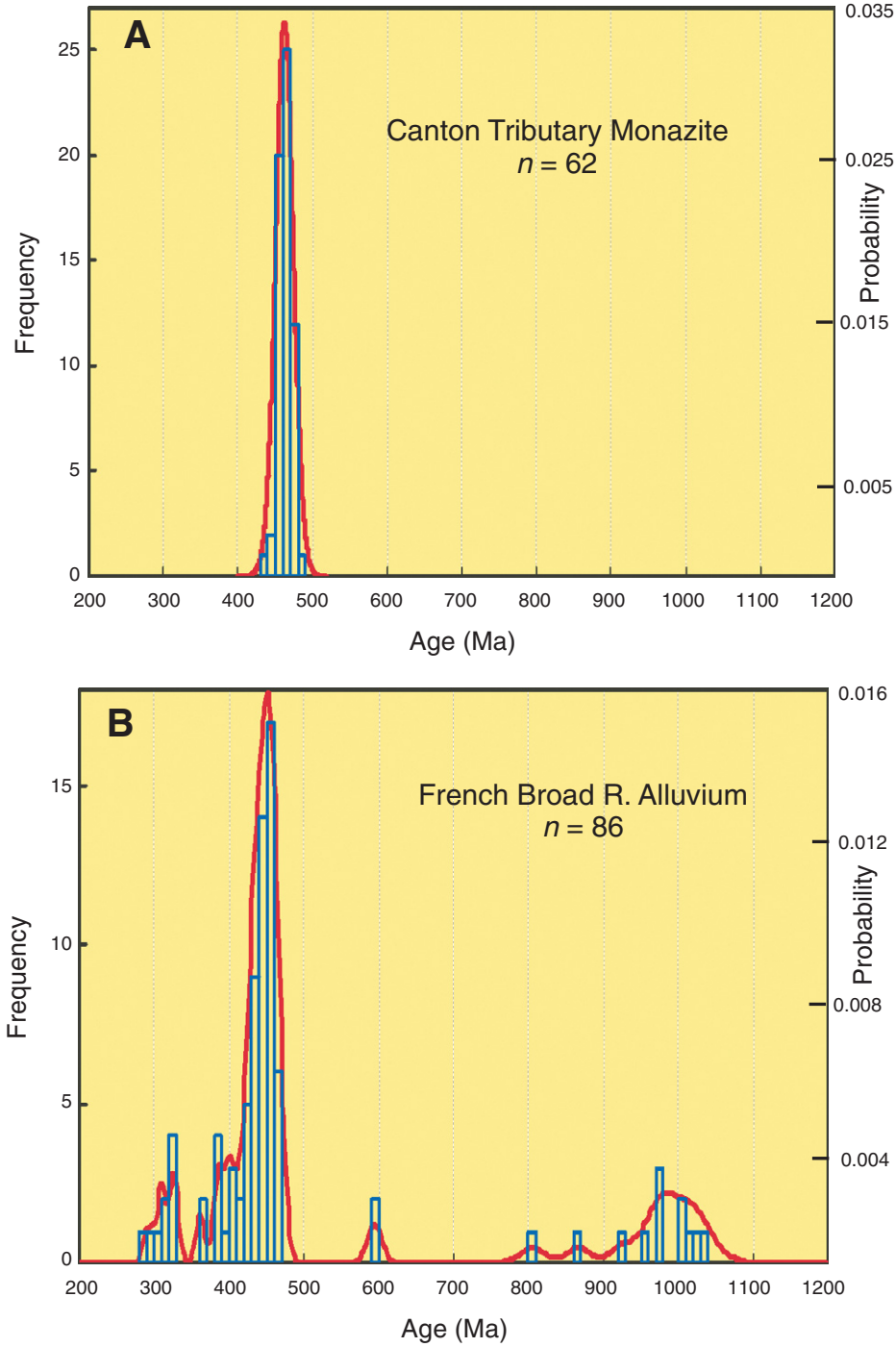

Figure 3. (A) Histogram compiling ^{232}Th-^{208}Pb ion microprobe ages for monazite from Canton quadrangle tributary streams derived from weathering of Mesoproterozoic gneisses and Neoproterozoic Ashe suite lithologies. (B) Histogram compiling all monazite analyses from French Broad River (R.) alluvium samples. Data are from Hietpas et al. (2010).

DISCUSSION

Age Distributions: Canton Tributaries versus French Broad River

The restricted sampling area of the Canton tributary streams (7.5 minute quadrangle [Merschat and Wiener, 1988]) compared to the wide region sampled by the French Broad River is reflected in both monazite and zircon age distributions. Based on abundance of monazite in Canton tributary and Ashe bedrock samples, it appears that Neoproterozoic metasedimentary rocks are the predominant source of monazite in this region of the Blue Ridge province, and the majority of the monazite is metamorphic. Either Ordovician monazite did not form in granitic Mesoproterozoic basement orthogneisses, or those rocks did not undergo Taconian metamorphism; the latter is unlikely, because basement lithologies are intimately interfolded with, and similarly migmatitic as, ATFS rocks that are at sillimanite grade. Although igneous monazite is difficult to distinguish from metamorphic monazite based solely on available ages or composition, given its abundance in ATFS rocks we argue that the monazite age mode in Figure 3 corresponds to the time of peak regional metamorphism.

Age Distributions: Monazite versus Zircon

The minor amount of Precambrian monazite is striking compared to the abundance of Paleozoic monazite (Fig. 3B). The Canton tributary samples illustrate the contrasting responsiveness of monazite in pelitic lithologies versus that in granitic systems during high-grade metamorphism. Apparently, there were no significant monazite-fertile pelitic lithologies among those composing the Mesoproterozoic basement complex, which is consistent with bedrock mapping in the region (Merschat and Cattanach, 2008).

In addition to compositional zoning patterns revealed by CL imaging (oscillatory zoning versus sector zoning versus no zoning), Th/U has been purported to distinguish magmatic zircon from metamorphic zircon. The Th/U value is usually higher in igneous zircon than metamorphic zircon. However, there is not a consensus as to the minimum value considered diagnostic of igneous zircon. Hoskin and Schaltegger (2003) stated that Th/U ≥ 0.5 is typical for igneous zircon, Vavra et al. (1999) stated that Th/U = 0.3 is typical of magmatic zircon, and Rubatto (2002) stated that magmatic zircon may have values as low as 0.18. For example, Mesoproterozoic magmatic zircon in igneous rocks from the Adirondack terrane, a classic locality for Grenville magmatism, has Th/U ranging from 0.1 to

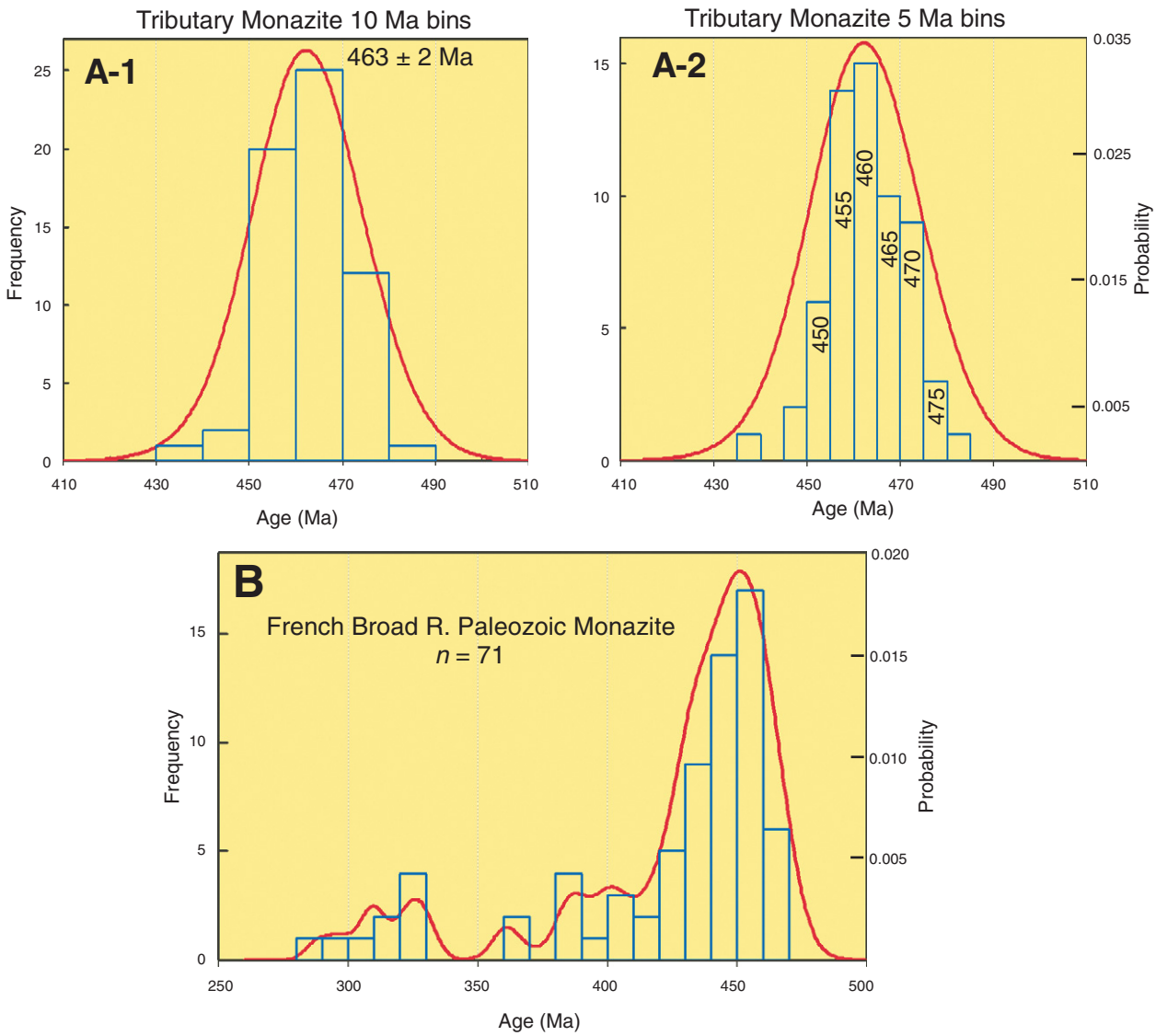

Figure 4. (A-1, A-2) Histograms and probability age distributions for only Ordovician monazite ages from tributary streams with 10 and 5 Ma bins. (B) All French Broad River (R.) Paleozoic monazites with 10 Ma bins. Data are from Hietpas et al. (2010).

1.5 (Fig. 6C). At upper amphibolite and granulite facies conditions under which anatexis is common, zircon in leucosomes is essentially magmatic (e.g., Moecher et al., 2004a), with Th/U values and zoning patterns indistinguishable from magmatic zircon.

The kyanite-sillimanite isograd is mapped in the Canton quadrangle, and much of the ATFS in the French Broad drainage is migmatitic (Fig. 2A), so some zircon growth is possible. Despite the high grade of metamorphism and onset of melt-forming reactions, tributary alluvium derived from weathering of Ashe lithologies, and direct samples of Ashe metasedimentary rocks, yield only a few Ordovician zircon ages, most of which are for zircon rims that have Th/U = 0.01–0.05 (Fig. 5F). Ashe bedrock and alluvium zircon remain dominated by Mesoproterozoic zircon ages in spite of the presence of widespread high-grade Middle Ordovician metamorphism and the abundance of Ordovician monazite ages.

Although the ranges of monazite and metamorphic zircon ages overlap for both tributary and French Broad River data sets, the peak of the dominant age populations for Ordovician metamorphic zircon in both the tributary and river alluvium samples is younger than the peak age of monazite (Figs. 4A, 5B, and 8A). Zircon and monazite need not date the same metamorphic reaction during a prograde event, and both ages inform our interpretation of the metamorphic history. Monazite growth has been shown to typically begin at lower amphibolite facies (staurolite grade) (Smith and Barreiro, 1990; Kingsbury et al., 1993; Foster et al., 2002; Wing et al., 2003; Gibson et al., 2004; Corrie and Kohn, 2008), whereas zircon growth typically coincides with the onset of partial melting (sillimanite grade and higher in metapelites) (Vavra et al., 1999; Rubatto et al., 2001; Moecher and Samson, 2006). For a high-grade terrane such as the southeastern Blue Ridge, monazite growth would begin early on the prograde P-T-t (pressure-temperature-time) path, but zircon growth would not begin until near the thermal peak of metamorphism, that is, later in the P-T-t path. A phase of monazite growth might occur

TABLE 4. ZIRCON AGE AND Th-U RATIOS, CANTON QUADRANGLE TRIBUTARY STREAMS

Sample No.	Th/U	Age (Ma)	Error (Ma)	Sample No.	Th/U	Age (Ma)	Error (Ma)
CT112 Ye (Zas)				**CT120 Ye, Zas**			
R9 G8 rim	0.28	441	5	R1 G8 CORE	0.36	1165	56
R10 G45 rim	0.09	447	4	R2 G13 CORE	0.41	1176	20
R10 G27 C	0.34	454	6	R2 G11 CORE	0.31	1191	90
R9 G8 Core B	0.06	704	7	R2 G39	0.33	1201	36
R10 G15	0.41	889	8	R2 G22	0.57	1229	47
R10 G32	0.58	1000	62	R2 G37	0.64	1229	21
R10 G8	0.34	1010	36	R2 G7 CORE	0.50	1249	23
R10 G16	0.31	1013	50	R2 G32	0.40	1288	19
R10 G13	0.41	1021	42	R2 G47	0.50	1491	31
R9 G6	0.28	1030	20	R2 G20 CORE	0.41	1500	34
R10 G29	0.34	1037	39	**CT141 Ye (Zas)**			
R10 G36	0.48	1048	58	R4 G38 TIP	0.18	424	13
R10 G47	0.25	1049	20	R3 G13	0.19	430	7
R9 G19	0.28	1060	31	R3 G30	0.22	430	12
R9 G41	0.60	1060	23	R4 G40 RIM	0.12	459	4
R10 G4	0.44	1070	43	R4 G39 LOW TIP	0.23	489	18
R9 G7	0.08	1079	23	R3 G17 UP TIP	0.13	577	12
R10 G45 core	0.10	1106	27	R3 G22 UP rim	0.04	916	19
R10 G5	0.47	1119	38	R3 G6	0.29	950	48
R10 G40 core	0.25	1152	36	R3 G3	0.82	999	56
R10 G3	0.26	1157	20	R4 G22 UP LFT RIM	0.12	1008	50
R10 G41	0.31	1158	20	R3 G4	0.69	1013	42
R10 G6	0.40	1164	20	R4 G39 CORE	0.36	1019	20
R9 G19	0.48	1173	86	R4 G24	0.35	1035	46
R9 G9	0.33	1174	26	R3 G35	0.12	1041	37
R9 G3	1.17	1178	60	R3 G23	0.28	1043	43
R10 G2	0.31	1184	20	R4 G38 CORE	0.36	1052	20
R9 G36	0.14	1189	30	R3 G16	0.33	1057	20
R9 G18	0.20	1196	39	R6 G23 UP RT	0.25	1202	23
R9 G25	0.61	1200	52	R5 G2 CORE	0.38	1203	27
R10 G9	0.42	1207	23	R5 G29	0.71	1203	41
R9 G29	0.19	1249	79	R5 G27	0.68	1227	43
R10 G25	0.20	1322	62	R5 G37 RHS	0.19	1256	23
R10 G23	0.29	1340	57	R5 G23 Core	0.32	1280	42
R9 G33	0.58	1696	54	**CT147 Zag**			
R10 G38	0.59	1781	34	R8 G2 RIM	0.04	425	11
CT120 Ye, Zas				R7 G1 Tip	0.06	429	4
R11 G14	0.83	994	25	R7 G14 LowTip	0.02	468	6
R2 G21 CORE	0.66	1024	32	R8 G38 TIP	0.05	470	12
R2 G31 CORE	0.44	1037	42	R8 G15	0.08	787	13
R2 G27	1.03	1056	43	R8 G19	0.14	874	15
R2 G54	0.77	1078	46	R8 G52	0.29	932	9
R2 G49	0.43	1094	20	R7 G1 Core	0.51	945	11
R2 G50	0.75	1114	20	R8 G29	0.26	957	95
R2 G44	0.25	1117	30	R7 G28	0.59	958	51
R2 G25	0.40	1126	77	R8 G32	0.27	981	44
R2 G53 CORE	0.30	1129	58	R7 G14Core	0.78	1009	38
R2 G26	0.54	1134	28	R8 G2 Core	0.17	1014	40
R2 G2	0.24	1141	56	R8 G43	0.20	1020	38
R2 G41	0.42	1142	40	R7 G33	0.43	1044	51
R2 G51	0.44	1158	33	R8 G1	0.44	1076	31

(*continued*)

as each successive isograd is reached (i.e., when prograde mineral reactions occur). Because lead diffusion in monazite is sufficiently slow (Cherniak et al., 2004), each phase of monazite growth would be preserved and is dateable if sufficient volume of monazite were generated by each event and resolvable by X-ray mapping techniques. Metamorphic zircon ages should be younger than most of the monazite ages in the same rock, with the youngest generation of monazite overlapping zircon growth. That is the pattern observed in the data set presented here, and emphasized by the range of monazite ages obtained by high spatial resolution electron microprobe chemical age dating. The most common ion probe and monazite chemical ages (460–465 Ma) are both slightly older than the dominant metamorphic zircon age population in our alluvial samples (ca. 455 Ma) and slightly older than the most precise ages for peak regional metamorphism in the Eastern Blue Ridge [concordant U-Pb zircon ID-TIMS age 458 ± 1 Ma (2σ) from granulite facies migmatites; Moecher et al., 2004a]. We propose that the 460–465 Ma monazite ages correspond to the time of the bulk of monazite growth that resulted from release of light rare earth elements from prograde allanite breakdown. The latter begins at lower amphibolite facies conditions, but before the metamorphic thermal peak (Smith and Barreiro, 1990; Wing et al., 2003; Corrie and Kohn, 2008).

Monazite Ion Microprobe versus Electron Microprobe Ages

Williams et al. (1999) demonstrated that monazite electron microprobe Th-U-Pb chemical ages are in many cases identical within uncertainty to conventional Th-U-Pb isotopic ages of monazite for the same rock, indicating that all of the assumptions of the EPMA technique are valid. The same outcome was obtained here when the same spots or growth zones were analyzed on the same crystals by both methods (Fig. 2B; Table 3). Based on ages discernable only by the order of magnitude higher spatial resolution of the electron microprobe, it is apparent that the monazite growth history, and by extension the metamorphic

TABLE 4. ZIRCON AGE AND Th-U RATIOS, CANTON QUADRANGLE TRIBUTARY STREAMS (*continued*)

Sample No.	Th/U	Age (Ma)	Error (Ma)	Sample No.	Th/U	Age (Ma)	Error (Ma)
CT147 Zag				**CT136 Zag**			
R8 G17	0.25	1099	76	R1 G8rim	0.02	447	6
R7 G7	0.07	1124	32	R2 G31 RIM	0.02	512	15
R8 G11	0.29	1127	31	R1 G7rim	0.20	745	18
R8 G27	0.19	1132	37	R2 G21rim	0.22	825	15
R7 G20	0.30	1135	36	R3 G26 CORE	0.54	1080	36
R8 G10	0.24	1145	46	R4 G35	0.78	1138	48
R8 G46	0.17	1151	66	R4 G41	1.46	1139	23
R8 G51	0.51	1154	44	R4 G47	0.43	1150	40
R7 G26	0.30	1176	55	R4 G36	0.38	1182	28
R8 G30	0.35	1184	44	R3 G15	0.41	1183	60
R7 G38	0.70	1192	68	R3 G2	1.07	1187	29
R8 G38 CORE	0.39	1195	87	R3 G22	0.66	1190	21
R8 G34	0.19	1287	44	R4 G23	0.59	1193	39
R7 G8	0.25	1296	44	R3 G28 CORE	1.71	1199	47
R8 G44	0.46	1299	35	R4 G34	0.47	1201	40
R7 G6	0.36	1299	64	R3 G7	0.48	1206	26
R11 G34	0.15	1006	40	R3 G1	0.23	1220	34
R11 G16	0.17	1011	28	R3 G21	0.30	1269	20
R11 G7	0.34	1047	20	R3 G43	0.99	1274	36
R11 G48	0.35	1061	50	R3 G8	0.39	1283	38
R11 G28	0.11	1090	65	R4 G40	0.94	1322	54
R12 G45	0.27	1109	20	R3 G12	0.52	1367	58
R11 G31	0.72	1111	27	R3 G11	0.30	1380	20
R11 G17	0.42	1131	20	**CT145 Zag**			
R11 G26	0.08	1142	20	R5 G29rim	0.06	417	12
R11 G47 TIP	0.14	1155	36	R6 G29rim	0.02	440	8
R11 G20	0.25	1160	31	R5 G33 rim	0.01	445	10
R11 G15	0.37	1161	20	R6 G31 rim	0.01	451	14
R12 G36	0.26	1172	20	R5 G23 rim	0.01	455	9
R12 G42	0.63	1188	20	R5 G2 rim	0.02	465	11
R11 G44	0.48	1194	20	R5 G22 rim	0.12	598	20
R11 G32	0.41	1198	20	R5 G8rim	0.23	774	27
R11 G38	0.40	1205	27	R6 G31	0.35	878	23
R11 G29	0.42	1214	63	R5 G1	1.50	971	9
R11 G4	0.50	1216	20	R5 G30	0.59	982	35
R11 G2	0.37	1219	26	R5 G13rim	0.08	985	42
R11 G37	1.06	1226	31	R5 G5	0.42	1028	33
R12 G47	0.63	1230	20	R5 G25	1.05	1049	58
R12 G44	0.24	1251	25	R5 G14	0.48	1055	74
R11 G33	0.20	1279	20	R5 G13 CORE	0.48	1057	74
R12 G35	2.25	1293	145	R5 G4 CORE	0.51	1116	64
R11 G6	0.49	1295	63	R5 G22 CORE	0.26	1149	42
R11 G11	0.94	1308	19	R5 G8 CORE	0.50	1157	32
R11 G25	0.58	1345	25	R5 G33 core	0.54	1182	27
R11 G18	0.53	1382	35	R5 G19	0.42	1194	39
R12 G41	0.45	1411	45	R8 G6	0.39	1312	19
R11 G23	0.61	1757	19	R8 G2 RIM	0.04	425	11
CT136 Zag				R8 G49	1.37	1364	208
R2 G11rim	0.02	423	12	R8 G22	0.24	1401	41
R2 G53rim	0.01	440	7				

Note: Grouped by bedrock lithologies in each tributary drainage basin (minor lithology in parentheses). Data from Hietpas et al. (2010).

history of the Blue Ridge, may be more complex than the history resolvable by monazite ion probe methods or zircon U-Pb geochronology. In addition to the dominant Middle Ordovician event, the electron microprobe revealed Middle to Late Cambrian, Early and Late Ordovician, Early Silurian, and Early Devonian monazite crystallization events. The ages correspond to known Appalachian tectonic phases and/or have age analogs among the zircon ages for the tributary samples and among the French Broad monazites.

The Th-U-Pb chemical ages for detrital monazite derived from ATFS paragneisses are the same as chemical, ion microprobe, and TIMS ages in Great Smoky Group schist and migmatitic gneisses to the southwest, which also probably formed from Neoproterozoic clastic rocks derived from Grenville sources (Zo map unit, Fig. 1B). Monazite chemical ages from the Great Smoky Group schist and gneiss define Early, Middle, and Late Ordovician ages (Moecher et al., 2004b, 2005), similar to EPMA and ion microprobe ages for monazite from the tributary stream samples. Some monazite grains contain late Neoproterozoic to early Paleozoic cores, and there are scattered younger ages within the distribution, similar to the pattern of French Broad monazite. Corrie and Kohn (2007) interpreted high mean square of weighted deviate values for U-Pb ID-TIMS analysis of monazite extracted from Great Smoky Group schists by microdrilling, spanning ages from 440 to 470 Ma, as not representing a single population of monazite growth. Corrie and Kohn (2007) established 450 ± 5 Ma as most closely representing the time of the majority of monazite growth, and by extension, the thermal peak of regional metamorphism in the Great Smoky Mountains region. These relations constitute preliminary evidence that Taconian regional metamorphism in the Appalachian Blue Ridge consisted of more than one tectonometamorphic pulse.

Henderson Orthogneiss

The age of the Henderson granite (Table 5), now dominantly an orthogneiss that is locally protomylonitic to ultramylonitic in the vicinity

TABLE 5. ZIRCON AGES FOR HENDERSON ORTHOGNEISS AND ASHE MIGMATITIC GNEISSES

Lithology/Analysis	Age (Ma)	Error (Ma)	Th/U	Lithology/Analysis	Age (Ma)	Error (Ma)	Th/U
Henderson Orthogneiss							
HENDr9gr30	446	9	1.14	HENDr9gr22	447	4	0.79
HENDr9gr29	445	22	0.85	HENDr9gr17	439	4	0.45
HENDr9gr27	442	4	0.56	HENDr9gr10rim	453	6	0.71
HENDr9gr26	467	6	0.47	HENDr9gr4	452	6	0.45
HENDr9gr25	455	5	0.51	HENDr9gr1	432	6	0.83
HENDr9gr23	455	5	0.61				
Ashe Mylonitic Gneiss							
FB4Br8gr20	1058	82	0.30	FB4Br8gr13	1145	81	0.24
FB4Br8gr19	1225	110	0.21	FB4Br8gr11	1115	60	0.41
FB4Br8gr18	1235	70	0.40	FB4Br8gr10	1068	53	0.14
FB4Br8gr17	1159	59	0.19	FB4Br8gr9	1194	95	0.43
FB4Br8gr16rim	1056	39	0.22	FB4Br8gr7	1052	67	0.29
FB4Br8gr16core	1020	78	0.52	FB4Br8gr6	1138	79	0.30
FB4Br8gr15	1057	97	0.27	FB4Br8gr5	1020	84	0.26
FB4Br8gr14rim	886	36	0.19	FB4Br8gr3RHS	1119	74	0.30
Ashe Migmatitic Gneiss							
ZAGr10gr1	1282	77	0.46	ZAGr10gr12core	1178	50	0.04
ZAGr10gr1lowrim	566	8	0.04	ZAGr10gr15	1147	92	1.15
ZAGr10gr2	1078	46	0.44	ZAGr10gr16	1031	45	0.24
ZAGr10gr4rim	463	4	0.01	ZAGr10gr17	463	9	0.01
ZAGr10gr4core	1227	53	1.01	ZAGr10gr18	939	24	0.38
ZAGr10gr5	582	47	0.24	ZAGr10gr24rim	445	5	0.01
ZAGr10gr6	756	22	0.28	ZAGr10gr26	986	61	0.86
ZAGr10gr7	923	10	0.19	ZAGr10gr27rim	449	7	0.02
ZAGr10gr8	870	21	0.10	ZAGr10gr27core	1019	36	0.25
ZAGr10gr10	1003	31	0.17	ZAGr10gr29	639	9	0.16
ZAGr10gr12	475	40	0.03	ZAGr10gr30	1015	61	0.24
Ashe Schist							
ZASr11gr2	1076	53	0.18	ZASr11gr19	955	39	0.37
ZASr11gr3	1199	50	0.61	ZASr11gr20	1056	81	0.23
ZASr11gr4	1034	56	0.08	ZASr11g21	1104	26	0.25
ZASr11gr5	1264	38	0.21	ZASr11gr22	1026	40	0.26
ZASr11gr8	1319	44	0.12	ZASr11gr24	883	19	0.25
ZASr11gr10	1262	31	0.33	ZASr11gr24b	880	21	0.30
ZASr11gr11	1272	64	0.20	ZASr11gr25	1034	24	0.40
ZASr11gr12	1142	47	0.34	ZASr11gr30	1324	23	0.36
ZASr11gr14	913	24	0.58	ZASr11gr35core	504	15	1.02
ZASr11gr15	1061	45	0.35	ZASr11gr35LTip	480	8	0.50
ZASr11gr18	1155	52	0.27	ZASr11gr37	1217	35	1.01

of the Brevard fault zone, is a long-standing problem in Blue Ridge tectonics (Horton and Butler, 1986). The Henderson is one of the largest exposed plutons in the southern Appalachians and probably was emplaced during a major period of granitic magmatism. U-Pb zircon and Rb-Sr isochron dates ranging from 600 to 350 Ma have been reported (e.g., Odom and Fullagar, 1973; Sinha and Glover, 1978), some of which are geologically meaningful. Carrigan et al. (2001) reported a SIMS microprobe U-Pb zircon age of ca. 490 Ma, but Vinson et al. (1999) reported ages for some zircon from the Henderson that are as young as 450 Ma. The concordia age determined here for a sample of Henderson gneiss is 447.6 ± 5.4 Ma, making the Henderson essentially a synmetamorphic Taconian pluton. If the Henderson were significantly older, or consisted of multiple plutons intruded over a span of time, older ages or a wider range of ages should be a prominent component of the alluvium zircon age distributions, as the French Broad headwaters flow across a region underlain almost exclusively by Henderson gneiss (Fig. 1B). The majority of Ordovician zircon from the alluvium samples is ca. 450 Ma with Th/U consistent with magmatic values (>>0.1; data in Hietpas et al., 2010) and with values measured for zircon from the rock sample of Henderson gneiss yielding the ca. 450 Ma age (Table 5).

Neoproterozoic Ages

Neoproterozoic zircon ages are rare but present in all zircon data sets (Figs. 5A, 6A, and 7A). Ages cluster in the ranges 600–550 and 800–700 Ma. As little new zircon was generated in the Ashe paragneisses, and most new zircon occurs as Ordovician rims on detrital Mesoproterozoic zircon, these zircons are most likely detrital and derived from Neoproterozoic rocks. The Th/U values for zircon younger than 800 Ma imply that both magmatic and metamorphic zircon is present (Fig. 7B).

The primary late Neoproterozoic tectonic event in the Blue Ridge was continental rifting, which is interpreted in the central and southern Appalachians to have involved two phases of rift-related magmatism (Crossnore plutonic-volcanic complex, Robertson River granites, Bakersville mafic intrusive suites; Catoctin and Mount Rogers volcanics) at 765–680 Ma and 620–550 Ma (Odom and Fullagar, 1984; Goldberg et al., 1986; Su et al., 1994; Aleinikoff et al., 1995; Tollo et al., 2004). These ages are well represented in French Broad River alluvium samples (Fig. 7A), particularly sample FB6 (data in Hietpas et al., 2010) collected northwest of Asheville in an area containing outcrops of Bakersville dikes (Rb-Sr isochron age of 734 ± 26 Ma; Goldberg et al., 1986). Although Crossnore type granites (U-Pb zircon crystallization ages of 745 ± 5 Ma: Su et al., 1994) do not crop out in the French Broad drainage basin, these rocks were apparently exposed and generating detrital zircon during deposition of ATFS sedimentary protoliths, as Neoproterozoic zircon ages also appear in tributary stream samples and ATFS gneisses.

Depositional Age of Ashe Metamorphic Suite Protoliths

The age distributions of Canton quadrangle tributary zircon and zircon from the sample of ATFS gneiss are very similar to detrital zircon age distributions of other extensive metaclastic rocks in the Western, Central, and Eastern Blue Ridge (Tallulah Falls Formation, Ocoee Supergroup, Coleman River Formation, Otto Formation, Chauga Belt rocks; Bream et al., 2004; Chakraborty et al., 2010). Based on regional bedrock mapping, Tallulah Falls Formation metasedimentary rocks are considered to be broadly time equivalent to Ashe Metamorphic Suite metasediments (Hatcher, 2002; Bream et al., 2004). The inferred equivalency is further supported by the new zircon data set presented here. The maximum depositional age of the Ashe suite protoliths is the age of the youngest detrital zircon, which must be as young as Cambrian, as indicated by the youngest zircon ages with magmatic Th/U values in the samples of ATFS gneiss (Figs. 5E, 5F; Table 5) and tributaries draining areas of ATFS bedrock (Fig. 5A). The maximum age of the Neoproterozoic Ocoee Supergroup, another Ashe suite correlative, based on the age of the Bakersville dikes intruding basement, and the absence of crosscutting relations with overlying Ocoee sediments, must be less than the age of the Bakersville dikes (ca. 735 Ma; Goldberg et al., 1986). This inference is supported by detrital zircon U-Pb ages for the lower Ocoee Supergroup (Wading Branch Formation) of 640 ± 10 Ma (Chakraborty et al., 2010) and diagenetic and/or metamorphic monazite and xenotime U-Pb ages of ca. 570–580 Ma for the Thunderhead Formation of the upper Ocoee Supergroup (Aleinikoff et al., 2010).

TABLE 6. AGES OF TRIBUTARY ZIRCONS FOR WHICH BOTH CORE AND RIM AGES WERE DETERMINED

Sample	Analysis	Th/U	Age (Ma)	Error (Ma)
CT112	R9 G8 rim	0.28	441	5
CT112	R9 G8 core	0.06	704	7
CT136	R2 G53 rim	0.01	440	7
CT136	R2 G53 core	0.30	1129	58
CT136	R1 G8 rim	0.02	447	6
CT136	R1 G8 core	0.36	1165	56
CT136	R2 G31 rim	0.02	512	15
CT136	R2 G31 core	0.44	1037	42
CT136	R2 G21 rim	0.22	825	15
CT136	R2 G21 core	0.66	1024	32
CT136	R2 G11 rim	0.02	423	12
CT136	R2 G11 core	0.31	1191	90
CT136	R1 G7 rim	0.20	745	18
CT136	R2 G7 core	0.50	1249	23
CT141	R4 G38 rim	0.18	424	13
CT141	R4 G38 core	0.36	1052	20
CT141	R3 G22 rim	0.04	916	19
CT141	R3 G22	0.66	1190	21
CT141	R4 G40 rim	0.12	459	4
CT141	R4 G40 core	0.94	1322	54
CT145	R6 G31 rim	0.01	451	14
CT145	R6 G31 core	0.35	878	23
CT145	R5 G29 rim	0.06	417	12
CT145	R5 G29 core	0.71	1203	41
CT145	R5 G33 rim	0.01	445	10
CT145	R5 G33 core	0.54	1182	27
CT145	R5 G23 rim	0.01	455	9
CT145	R5 G23 core	0.32	1280	42
CT147	R7 G1 rim	0.06	429	4
CT147	R7 G1 core	0.51	945	11
CT147	R8 G2 rim	0.04	425	11
CT147	R8 G2 core	0.17	1014	40
CT147	R7 G14 rim	0.02	468	6
CT147	R7 G14 core	0.78	1009	38
CT147	R8 G38 rim	0.05	470	12
CT147	R8 G38 core	0.39	1195	87

IMPLICATIONS FOR SOUTHERN BLUE RIDGE TECTONICS

The monazite and zircon geochronology presented here corroborates the emerging pattern of metamorphic crystallization and cooling ages in the Southern Blue Ridge. Although Paleozoic orogenesis was a temporally protracted process in the Western and Eastern Blue Ridge in North Carolina, peak Barrovian regional metamorphism northwest of the Brevard zone, as bracketed by ages of metamorphic monazite (growth on the prograde path or at the thermal peak) and ages of zircon rims on Mesoproterozoic zircon cores in metasedimentary rocks (growth at the thermal peak), is definitively Middle Ordovician (Taconian). In contrast, regional metamorphism in the western Inner Piedmont is distinctly younger (Late Devonian to Mississippian; Dennis, 2007); evidence for this includes monazite ID-TIMS U-Pb geochronology (Dennis and Wright, 1997), and SIMS U-Pb ages of zircon rims (Carrigan et al., 2001) in orthogneisses and metasediments of the western Inner Piedmont that are correlated with the Tallulah Falls Formation of the Eastern Blue Ridge (Hatcher, 2002). Middle Paleozoic zircon rim ages are also found in easternmost Blue Ridge rocks near the Brevard fault zone (Carrigan et al., 2001). Albeit much less abundant than Ordovician monazite, most of the late Paleozoic monazite ages in our data set are for monazite grains in alluvium samples collected on the southeast side of the Brevard fault zone. Although the age of the metamorphic peak is different in the Eastern Blue Ridge and western Inner Piedmont, there is abundant evidence for middle and late Paleozoic retrograde metamorphism in the Eastern Blue Ridge (Goldberg and Dallmeyer, 1997; Moecher et al., 2007; Miller et al., 2010), but as yet no evidence for Ordovician metamorphism in the western Inner Piedmont (Dennis, 2007). The only non-Ordovician monazite age in the tributary data set (definitive Eastern Blue Ridge affinity) is from a thin monazite rim detected by high spatial resolution EPMA (Fig. 2B). The pattern and distribution of ages suggest variable and nonpenetrative overprinting of Taconian fabrics and mineral assemblages by younger deformation that is progressively more pervasive to the southeast. Resolution of the manner in which middle to late Paleozoic tectonometamorphism characteristic of the western Inner Piedmont overprinted early Paleozoic effects in the Eastern Blue Ridge would be facilitated by an extensive program of ion probe isotopic analysis and microprobe chemical age dating of rocks across the Brevard fault zone, in the context of the deformation and retrograde metamorphic history of those rocks.

Published ^{40}Ar-^{39}Ar hornblende and muscovite age distributions provide further evidence for this contrasting thermotectonic history for the Eastern Blue Ridge and western Inner Piedmont. Many hornblende ^{40}Ar-^{39}Ar age spectra for Eastern Blue Ridge rocks in western North Carolina fail to define plateaus, suggesting isotopic disturbance (Goldberg and Dallmeyer, 1997), but the few samples that define plateaus yield Ordovician to Silurian ages (Dallmeyer, 1975; Kunk et al., 2006). In contrast, hornblende cooling ages in the westernmost Inner Piedmont (including the Brevard zone) are latest Devonian to Carboniferous (Dallmeyer, 1988), decreasing to Permian in the eastern Inner Piedmont (Dallmeyer et al., 1986). The late Paleozoic hornblende ages are derived from Ar release spectra that generally define plateaus, in contrast to the large degree of disturbance in Eastern Blue Ridge rocks along strike to the northeast. Exceptions to the pattern of disturbed Eastern Blue Ridge hornblende age spectra are the plateau ages of 354 and 362 Ma for the Lake Chatuge mafic-ultramafic complex (LCC, Fig. 1A) in the Eastern Blue Ridge of southernmost North Carolina and northernmost Georgia (Fig. 1A) (Dallmeyer, 1989). Muscovite plateau ^{40}Ar-^{39}Ar ages for schists, gneisses, and retrograde mylonites in the Eastern Blue Ridge tend to have an older upper age limit (370–320 Ma; Connelly and Dallmeyer, 1993; Goldberg and Dallmeyer, 1997; Kunk et al., 2006) than western Inner Piedmont muscovites (Dallmeyer, 1988) (Fig. 10).

Although inferred to not be a suture (Hatcher, 2002), based primarily on the similarity of detrital zircon age distributions in metasedimentary rocks from its contiguous belts (Bream et al., 2004), the Brevard fault zone is clearly a significant tectonic boundary separating rocks of different metamorphic age, grade, structural style, and igneous composition (Miller et al., 2000; Mapes et al., 2001; Merschat et al., 2005; Dennis, 2007). The ductile, peak metamorphic (sillimanite grade), and largely strike-slip component of motion on the Brevard fault zone (Reed and Bryant, 1964; Vauchez, 1987) cannot explain the contrast, requiring a component of significant Pennsylvanian vertical displacement, as indicated by the difference in muscovite cooling ages between the western Blue Ridge and western Inner Piedmont (Fig. 10). The Rosman fault, a late southeast-dipping thrust fault within the Brevard fault zone (Horton and Butler, 1986), may accommodate some of the requisite displacement.

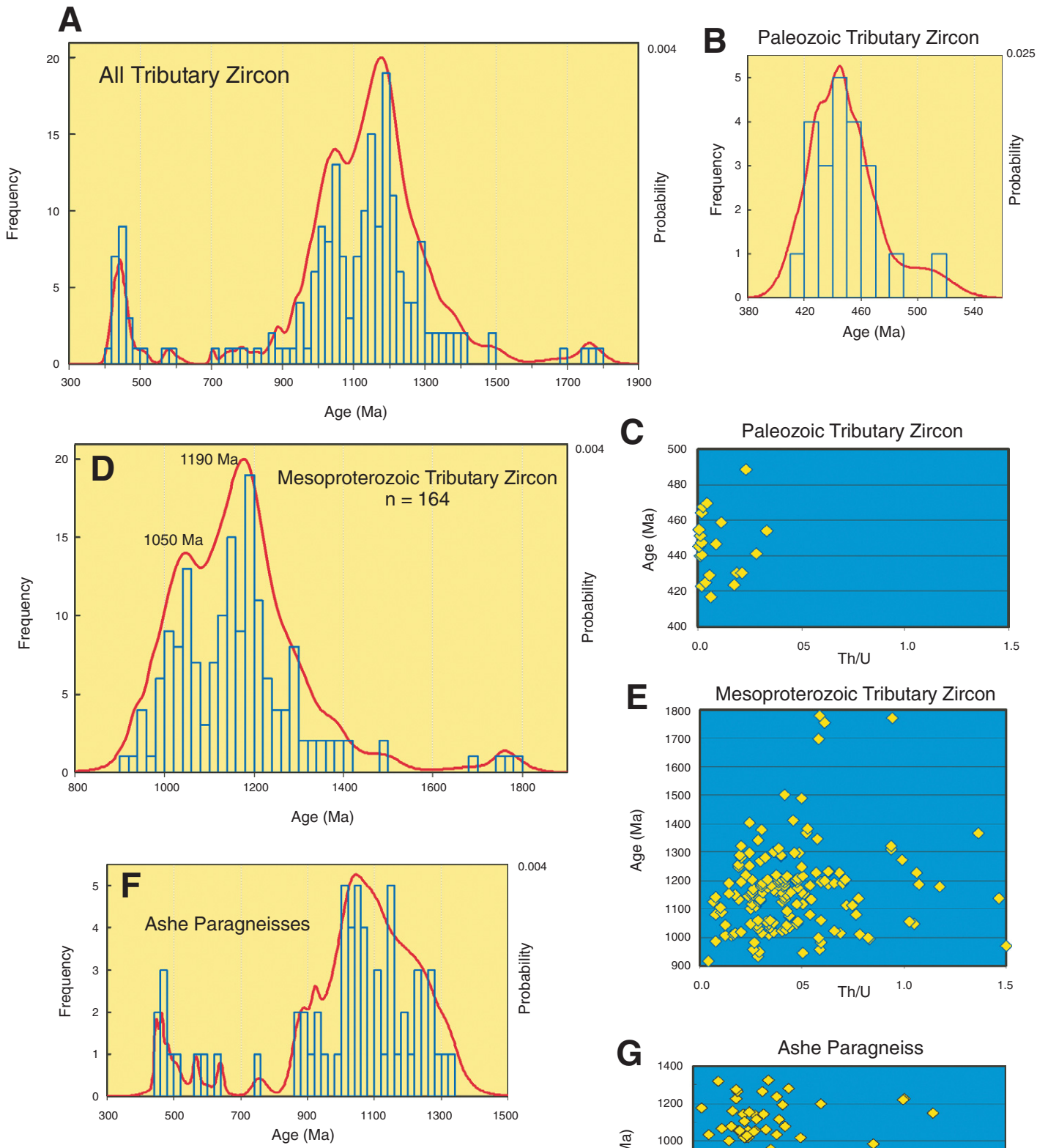

Figure 5. (A) Histogram of all zircon ages for Canton quadrangle tributary streams. (B) Histogram of Paleozoic zircons in A. (C) Values of Th/U for zircons in B. (D) Age histogram, probability age distribution, and dominant age peaks for Mesoproterozoic zircons in A. (E) Values of Th/U for Mesoproterozoic zircon in D. (F, G) Ages and Th/U for zircon from Ashe suite migmatitic paragneisses. Data in A–E are from Hietpas et al. (2010); data for F and G are in Table 5.

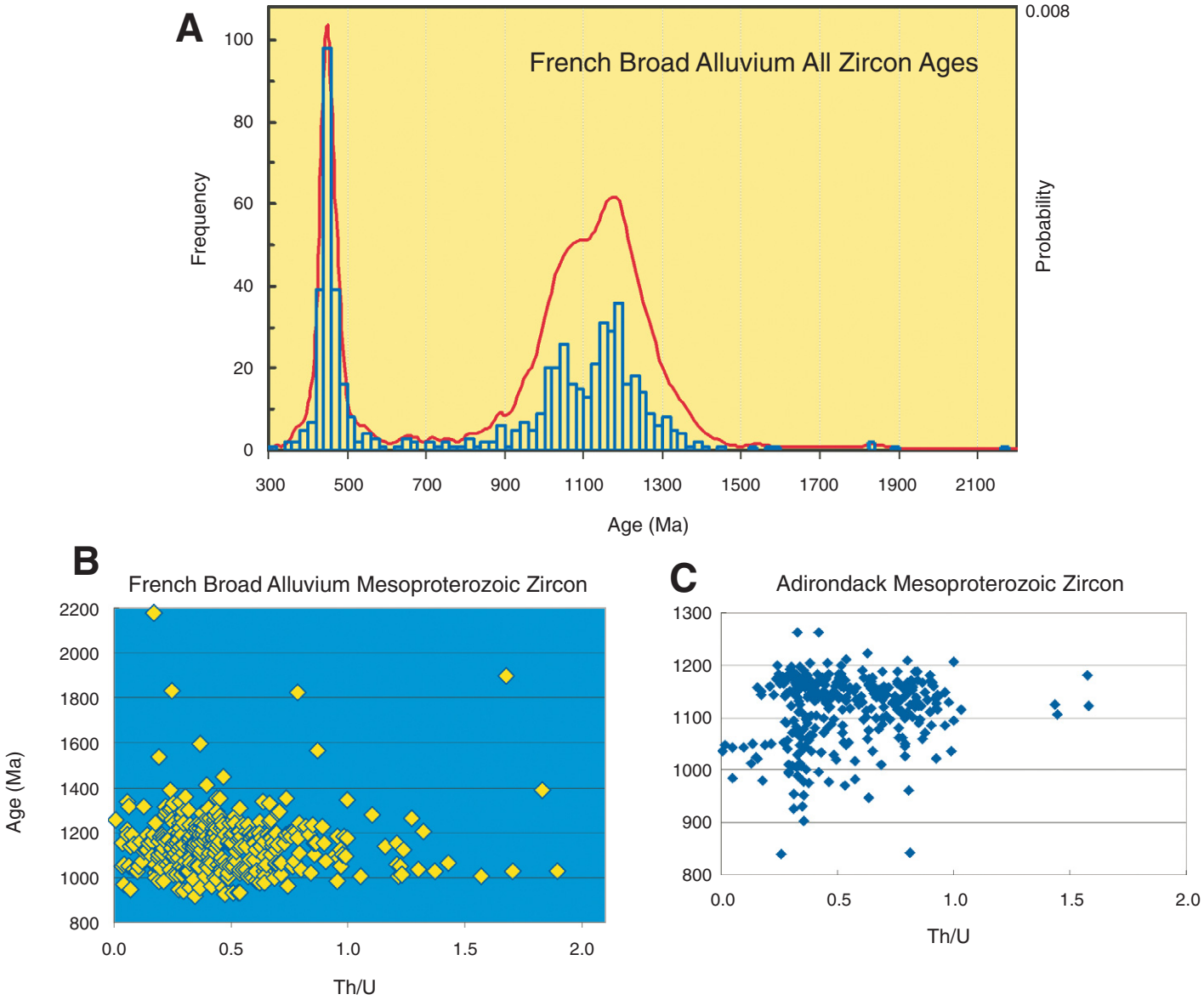

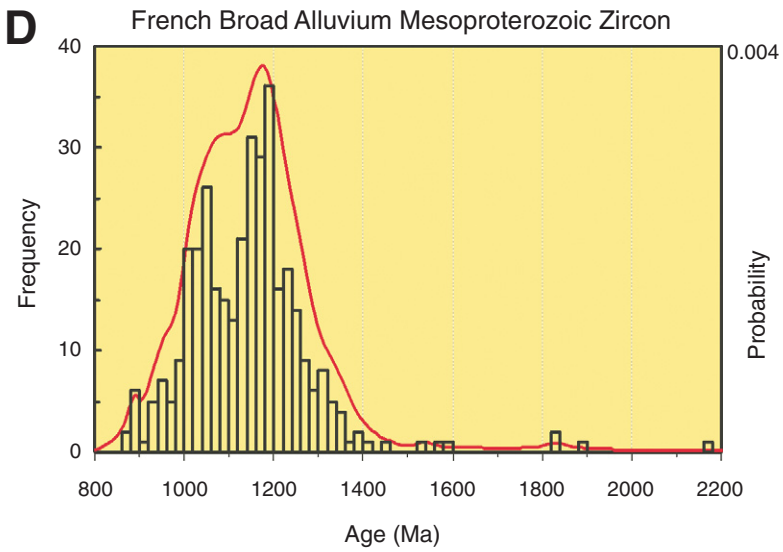

Figure 6. (A) Age histogram for all zircon from French Broad River alluvium. (B) Th/U for Mesoproterozoic zircon in alluvium. (C) Th/U for zircon from Adirondack AMCG (anorthosite-mangerite-charnockite-granite) suite rocks (data from McLelland et al., 2004). (D) Age histogram for Mesoproterozoic zircon only. Data in A, B, D are from Hietpas et al. (2010).

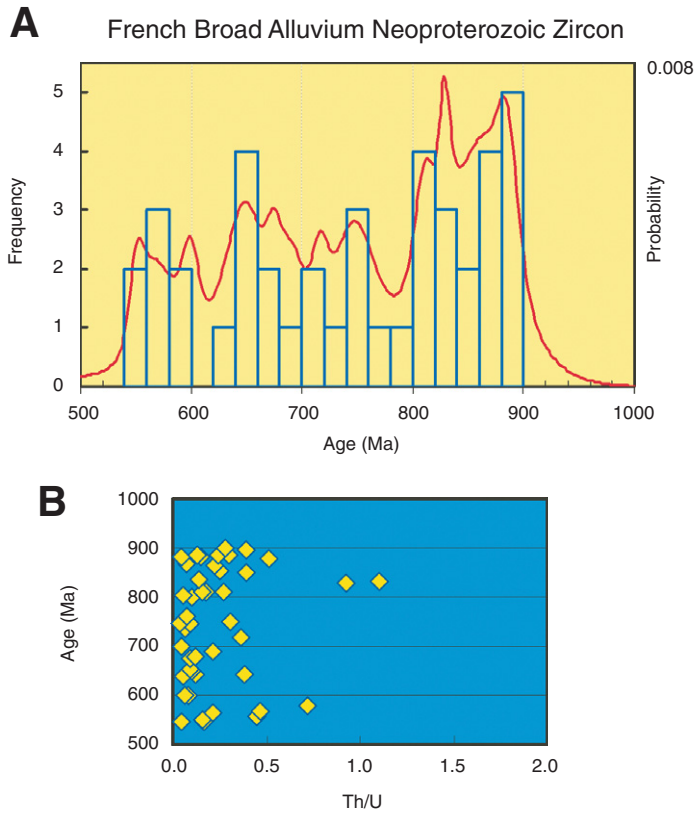

Figure 7. Neoproterozoic zircon from French Broad River alluvium. (A) Age histogram. (B) Th/U values.

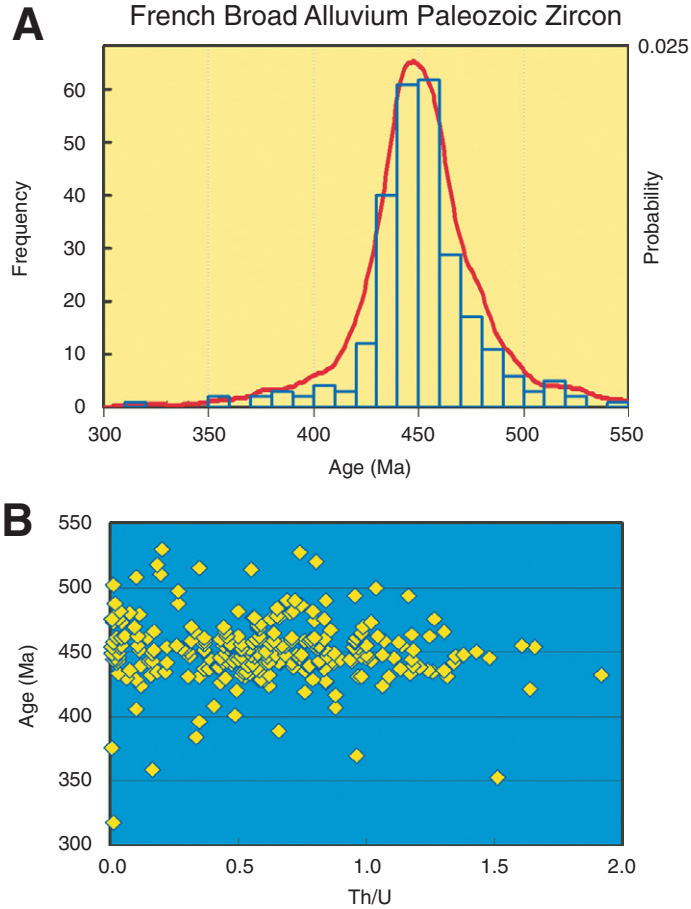

Figure 8. Paleozoic zircon from French Broad alluvium. (A) Age histogram. (B) Th/U values. Data are from Hietpas et al. (2010).

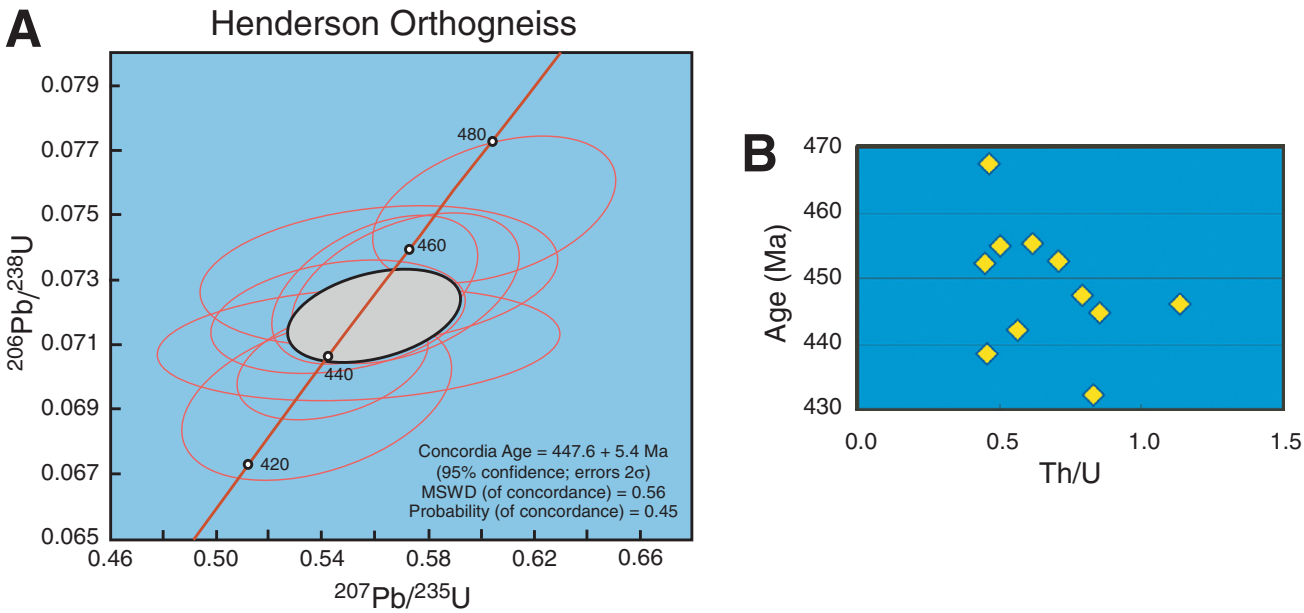

Figure 9. Concordia diagram and age for sample of Henderson orthogneiss, western Inner Piedmont, collected from an outcrop at alluvium sample site FB4 (see Fig. 1). MSWD—mean square of weighted deviates.

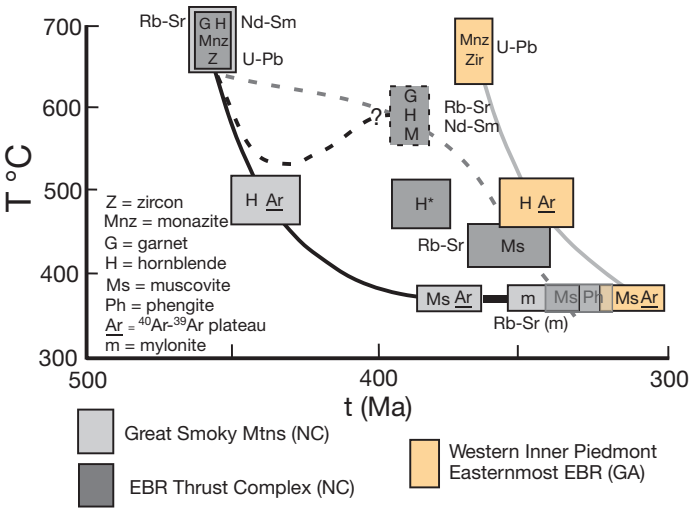

Figure 10. Comparative temperature-time (T, t) histories for three regions of Southern Blue Ridge in western North Carolina (NC), northeast Georgia (GA), and western South Carolina that are partially within or adjacent to French Broad River drainage basin. EBR—Eastern Blue Ridge. Data sources: this study, Dallmeyer (1988), Goldberg and Dallmeyer (1997), Kunk et al. (2006), Moecher et al. (2004a, 2004b, 2005), Merschat et al. (2006), Corrie and Kohn (2007), Dennis and Wright (1997). Asterisk indicates hornblende ages of Goldberg and Dallmeyer (1997) based on disturbed ^{40}Ar-^{39}Ar isotopic systematics.

SUMMARY

Peak Barrovian regional metamorphism in the Western and Eastern Blue Ridge of the southern Appalachian orogen, as determined by high spatial resolution analysis methods on monazite and zircon in alluvium and bedrock samples, is Middle Ordovician. Details of age distributions and the highest spatial resolution age measurements reveal that tectonometamorphism occurred in three phases that span the Ordovician Period. There is thus a richer history of events that requires deconvolution by microgeochronology in order to construct a more complete and accurate tectonic model for the Taconian.

Lithologically, the Southern Blue Ridge is a relatively magma poor region, dominated by extensive latest Neoproterozoic to Cambrian metaclastic sequences. The fingerprint of the orogen, from a detrital mineral provenance perspective, is dominated by Mesoproterozoic zircon derived from basement that exhibits a very weak response to Paleozoic metamorphism. Monazite in selected lithologies is much more responsive to regional tectonometamorphic events. As both minerals have strengths and limitations as a provenance indicator, a more informative approach to provenance analysis would involve routine analysis of both detrital monazite and detrital zircon. The availability of high throughput microanalysis systems now makes such an approach highly practicable.

ACKNOWLEDGMENTS

We thank Axel Schmitt for supervising the secondary ion mass spectrometry analytical sessions at the University of California, Los Angeles, and for guidance on interpretation of analyses, Victor Valencia for supervising analytical sessions at the University of Arizona LaserChron center, and Mike Jercinovic (University of Massachusetts) for supervising monazite electron probe microanalysis. We also thank Doug Rankin, Calvin Miller, and Brent Miller for helpful critical reviews of the manuscript. This research was supported by National Sciences Foundation grants EAR-0635688, EAR-0001322, EAR-0635643, and EAR-0447154.

REFERENCES CITED

Absher, S.A., and McSween, H.Y., 1985, Granulites at Winding Stair Gap, North Carolina: The thermal axis of Paleozoic metamorphism in the southern Appalachians: Geological Society of America Bulletin, v. 96, p. 588–599, doi: 10.1130/0016-7606(1985)96<588:GAWSGN>2.0.CO;2.

Aleinikoff, J.N., Zartman, R.E., Walter, M., Rankin, D.W., Lyttle, P.T., and Burton, W.C., 1995, U-Pb ages of metarhyolites of the Catoctin and Mount Rogers Formations, central and southern Appalachians: Evidence for two pulses of Iapetan rifting: American Journal of Science, v. 295, p. 428–454, doi: 10.2475/ajs.295.4.428.

Aleinikoff, J.N., Southworth, S., and Kunk, M.J., 2007, SHRIMP U-Pb geochronology of zircon and titanite and ^{40}Ar/^{39}Ar of hornblende and muscovite from Mesoproterozoic rocks of the western Blue Ridge, Great Smoky Mountains National Park area, TN and NC: Geological Society of America Abstracts with Programs, v. 39, no. 2, p. 78.

Aleinikoff, J.N., Southworth, S., Fanning, C.M., and Mazdab, F.K., 2010, Evidence for late Neoproterozoic deposition of the Ocoee Supergroup: SHRIMP U-Pb and trace element analysis of diagenetic xenotime and monazite: Geological Society of America Abstracts with Programs, v. 42, p. 59.

Bream, B.R., Hatcher, R.D., Jr., Miller, C.F., and Fullagar, P.D., 2004, Detrital zircon ages and Nd isotopic data from the southern Appalachian crystalline core, Georgia, South Carolina, North Carolina, and Tennessee: New provenance constraints for part of the Laurentian margin, *in* Tollo, R.P., et al., eds., Proterozoic tectonic evolution of the Grenville orogen in North America: Geological Society of America Memoir 197, p. 459–475, doi: 10.1130/0-8137-1197-5.459.

Butler, R.D., 1973, Paleozoic deformation and metamorphism in part of the Blue Ridge thrust sheet, North Carolina: American Journal of Science, v. 273-A, p. 72–88.

Carpenter, R.H., 1970, Metamorphic history of the Blue Ridge province of Tennessee and North Carolina: Geological Society of America Bulletin, v. 81, p. 749–762, doi: 10.1130/0016-7606(1970)81[749:MHOTBR]2.0.CO;2.

Carrigan, C.W., Bream, B.R., Miller, C.F., and Hatcher, R.D., 2001, Ion microprobe analyses of zircon rims from the eastern Blue Ridge and Inner Piedmont, NC-SC-GA: Implications for the timing of Paleozoic metamorphism in the southern Appalachians: Geological Society of America Abstracts with Programs, v. 33, no. 2, p. A-7.

Carrigan, C.W., Miller, C.F., Fullagar, P.D., Bream, B.R., Hatcher, R.D., Jr., and Coath, C.D., 2003, Ion microprobe age and geochemistry of southern Appalachian basement, with implications for Proterozoic and Paleozoic reconstructions: Precambrian Research, v. 120, p. 1–36, doi: 10.1016/S0301-9268(02)00113-4.

Chakraborty, S., Moecher, D.P., Samson, S.D., and Loughry, D., 2010, Provenance analysis of the Neoproterozoic Ocoee Supergroup eastern Great Smokey Mountaions, NC/TN: Geological Society of America Abstracts with Program, v. 42, no. 1, p. 58.

Cherniak, D.J., Watson, E.B., Grove, M., and Harrison, T.M., 2004, Pb diffusion in monazite: A combined RBS/SIMS study: Geochimica et Cosmochimica Acta, v. 68, p. 829–840, doi: 10.1016/j.gca.2003.07.012.

Clemons, K.M., and Moecher, D.P., 2009, Reinterpretation of the deformation history of the Greenbrier fault, Great Smoky Mountains: Petrologic, structural, and geochemical constraints: Geological Society of America Bulletin, v. 121, p. 1108–1122, doi: 10.1130/B26480.1.

Connelly, J.B., and Dallmeyer, R.D., 1993, Polymetamorphic evolution of the western Blue Ridge: Evidence from ^{40}Ar-^{39}Ar whole-rock slate/phyllite and muscovite ages: American Journal of Science, v. 293, p. 322–359, doi: 10.2475/ajs.293.4.322.

Corfu, F., Hanchar, J., Hoskin, P., and Kinny, P., 2003, Atlas of zircon textures, *in* Hanchar, J.M. and Hoskin, P.W.O., eds., Zircon: Reviews in Mineralogy and Geochemistry, v. 53, p. 469–500.

Corrie, S.L., and Kohn, M.J., 2007, Resolving the timing of orogenesis in the western Blue Ridge, southern Appalachians via in situ ID-TIMS monazite geochronology: Geology, v. 35, p. 627–630, doi: 10.1130/G23601A.1.

Corrie, S.L., and Kohn, M.J., 2008, Trace-element distributions in silicates during prograde metamorphic reactions: Implications for monazite formation: Journal of Metamorphic Geology, v. 26, p. 451–464, doi: 10.1111/j.1525-1314.2008.00769.x.

Dallmeyer, R.D., 1975, ^{40}Ar-^{39}Ar ages of biotite and hornblende from a progressively remetamorphosed basement terrane: Their bearing on interpretation of release spectra: Geochimica et Cosmochimica Acta, v. 39, p. 1655–1669, doi: 10.1016/0016-7037(75)90087-3.

Dallmeyer, R.D., 1988, Late Paleozoic tectonothermal evolution of the western Piedmont and eastern Blue Ridge, Georgia: Controls on the chronology of terrane accretion and transport in the southern Appalachian orogen:

Geological Society of America Bulletin, v. 100, p. 702–713, doi: 10.1130/0016-7606(1988)100<0702:LPTEOT>2.3.CO;2.

Dallmeyer, R.D., 1989, ^{40}Ar-^{39}Ar geochronology within the eastern Blue Ridge, *in* Dallmeyer, R.D., ed., Tectonostratigraphic expression of terrane accretion in the Southern Appalachian Orogen: A geotraverse excursion: IGCP Project 233, Terranes in the Circum-Atlantic Paleozoic Orogens, p. 7-10–7-21.

Dallmeyer, R.D., Wright, J.E., Secor, D.T., Jr., and Snoke, A.W., 1986, Character of Alleghanian orogeny in the southern Appalachians: Part II: Geochronological constraints on the tectonothermal evolution of the eastern Piedmont in South Carolina: Geological Society of America Bulletin, v. 97, p. 1329–1344, doi: 10.1130/0016-7606(1986)97<1329:COTAOI>2.0.CO;2.

Dennis, A.J., 2007, Cat Square basin, Catskill clastic wedge: Silurian-Devonian orogenic events in the central Appalachians and the crystalline southern Appalachians, *in* Sears, J.W., et al., eds., Whence the Mountains? Inquires into the evolution of orogenic systems: A volume in honor of Raymond A. Price: Geological Society of America Special Paper 433, p. 313–329, doi: 10.1130/2007.2433(15).

Dennis, A.J., and Wright, J.E., 1997, Middle and late Paleozoic monazite U-Pb ages, Inner Piedmont, South Carolina: Geological Society of America Abstracts with Programs, v. 29, no. 3, p. 12.

DeWolf, C.P., Zessler, C.J., Halliday, A.N., Mezger, K., and Essene, E.J., 1996, The role of inclusions in U-Pb and Sm-Nd garnet chronology: Stepwise dissolution experiments and trace uranium mapping by fission track analysis: Geochimica et Cosmochimica Acta, v. 60, p. 121–134, doi: 10.1016/0016-7037(95)00367-3.

Eckert, J.O., Jr., Hatcher, R.D., Jr., and Mohr, D.W., 1989, The Wayah granulite facies metamorphic core, southwestern North Carolina: High grade culmination of Taconic metamorphism in the southern Blue Ridge: Geological Society of America Bulletin, v. 101, p. 1434–1447, doi: 10.1130/0016-7606(1989)101<1434:TWGFMC>2.3.CO;2.

Foster, G., Gibson, H.D., Parrish, R., Horstwood, M., Fraser, J., and Tindle, A., 2002, Textural, chemical, and isotopic insights into the nature and behavior of metamorphic monazite: Chemical Geology, v. 191, p. 183–207, doi: 10.1016/S0009-2541(02)00156-0.

Gehrels, G., Valencia, V., and Ruiz, J., 2008, Enhanced precision, accuracy, efficiency, and spatial resolution of U-Pb ages by laser ablation-multicollector-inductively coupled plasma-mass spectrometry: Geochemistry Geophysics Geosystems, v. 9, p. 1–13, doi: 10.1029/2007GC001805.

Gibson, H.D., Carr, S.D., Brown, R.L., and Hamilton, M.A., 2004, Correlations between chemical and age domains in monazite, and metamorphic reactions involving major pelitic phases: An integration of ID-TIMS and SHRIMP geochronology with Y-Th-U X-ray mapping: Chemical Geology, v. 211, p. 237–260, doi: 10.1016/j.chemgeo.2004.06.028.

Goldberg, S.A., and Dallmeyer, R.D., 1997, Chronology of Paleozoic metamorphism and deformation in the Blue Ridge thrust complex, North Carolina and Tennessee: American Journal of Science, v. 297, p. 488–526, doi: 10.2475/ajs.297.5.488.

Goldberg, S.A., Butler, J.R., and Fullagar, P.D., 1986, The Bakersville dike swarm: Geochronology and petrogenesis of Late Proterozoic basaltic magmatism in the southern Appalachian Blue Ridge: American Journal of Science, v. 286, p. 403–430, doi: 10.2475/ajs.286.5.403.

Grove, M., Jacobson, C., Barth, A., and Vucic, A., 2003, Temporal and spatial trends of Late Cretaceous–early Tertiary underplating Pelona and related schist beneath southern California and southwestern Arizona, *in* Johnson, S.E., et al, eds., Tectonic evolution of northwestern Mexico and the southwestern USA: Geological Society of America Special Paper 374, p. 381–406, doi: 10.1130/0-8137-2374-4.381.

Hadley, J.D., and Goldsmith, R., 1963, Geology of the eastern Great Smoky Mountains, North Carolina and Tennessee: U.S. Geological Survey Professional Paper 349-B, 118 p.

Hadley, J.D., and Nelson, A.E., 1971, Geologic map of the Knoxville quadrangle, North Carolina, Tennessee, and South Carolina: U.S. Geological Survey Miscellaneous Geological Investigations Map I-654, scale 1:250,000.

Hanchar, J.M., and Miller, C.F., 1993, Zircon zonation patterns as revealed by cathodoluminescence and backscattered electron images: Chemical Geology, v. 110, p. 1–13, doi: 10.1016/0009-2541(93)90244-D.

Harrison, T.M., McKeegan, K., and LeFort, P., 1995, Detection of inherited monazite in the Manaslu leucogranite by ^{232}Th-^{208}Pb ion microprobe dating: Crystallization age and tectonic implications: Earth and Planetary Science Letters, v. 133, p. 271–282, doi: 10.1016/0012-821X(95)00091-P.

Hatcher, R.D., Jr., 1978, Tectonics of the western Piedmont and Blue Ridge, southern Appalachians: Review and speculation: American Journal of Science, v. 278, p. 276–304, doi: 10.2475/ajs.278.3.276.

Hatcher, R.D., Jr., 1987, Tectonics of the southern and central Appalachian internides: Annual Review of Earth and Planetary Sciences, v. 15, p. 337–362, doi: 10.1146/annurev.ea.15.050187.002005.

Hatcher, R.D., Jr., 2002, An Inner Piedmont primer, *in* Hatcher, R.D., Jr., and Bream, B.R., eds., Inner Piedmont geology in the South Mountains–Blue Ridge Foothills and the southwestern Brushy Mountains, central-western North Carolina: Carolina Geological Society Annual Field Trip Guidebook 2002, p. 1–18.

Hatcher, R.D., Jr., 2005, A Blue Ridge Primer, *in* Hatcher, R.D., Jr., and Merschat, A.J., eds., Blue Ridge geology geotraverse east of the Great Smoky Mountains National Park, western North Carolina: Carolina Geological Society Annual Field Trip Guidebook 2005, p. 1–18.

Hawkins, D.P., and Bowring, S.A., 1997, U-Pb systematics of monazite and xenotime; case studies from the Paleoproterozoic of the Grand Canyon, Arizona: Contributions to Mineralogy and Petrology, v. 127, p. 87–103, doi: 10.1007/s004100050267.

Hietpas, J., Samson, S.D., Moecher, D.P., and Schmitt, A., 2010, Detrital monazite plays in high fidelity: Geology, v. 38, p. 167–170, doi: 10.1130/G30265.1.

Horton, J.W., and Butler, J.R., 1986, The Brevard fault zone at Rosman, Transylvania County, North Carolina, *in* Neathery, T.L., ed., Centennial Field Guide, Southeastern Section: Geological Society of America Centennial Field Guide Volume 6, p. 251–256.

Hoskin, P.W.O., and Schaltegger, U., 2003, The composition of zircon and igneous and metamorphic petrogenesis, *in* Hanchar, J.M., and Hoskin, P.W.O., eds., Zircon: Reviews in Mineralogy and Geochemistry, v. 53, p. 27–62.

Kingsbury, J.A., Miller, C.F., Wooden, J.L., and Harrison, T.M., 1993, Monazite paragenesis and U-Pb systematic in rocks of the eastern Mojave Desert, California, U.S.A.: Implications for thermochronometry: Chemical Geology, v. 110, p. 147–167, doi: 10.1016/0009-2541(93)90251-D.

Kretz, R., 1983, Symbols for rock-forming minerals: American Mineralogist, v. 68, p. 277–279.

Kunk, M.J., Southworth, S., Aleinikoff, J.N., Naeser, N.D., Naeser, C.W., Merschat, C.E., and Cattanach, B.L., 2006, Preliminary U-Pb, ^{40}Ar-^{39}Ar, and fission-track ages support a long complex tectonic history in the western Blue Ridge in North Carolina and Tennessee: Geological Society of America Abstracts with Programs, v. 38, no. 3, p. 66.

Lanzirotti, A., and Hanson, G.N., 1995, U-Pb dating of major and accessory minerals formed during metamorphism and deformation of metapelites: Geochimica et Cosmochimica Acta, v. 59, p. 2513–2526, doi: 10.1016/0016-7037(95)00146-8.

Mapes, R.W., Miller, C.F., Fullager, P.D., and Bream, B.R., 2001, Acadian plutonism in the Inner Piedmont and eastern Blue Ridge, North Carolina and northern Georgia: Geological Society of America Abstracts with Programs, v. 33, no. 2, p. 30.

Massey, M.A., and Moecher, D.P., 2005, Metamorphic, structural, and fabric evolution of a segment of the Eastern Blue Ridge–Western Blue Ridge boundary in central western North Carolina: Tectonics, v. 24, TC4010, doi: 10.1029/2004TC001643.

McLelland, J.M., Bickford, M.E., Hill, B.M., Clechenko, C.C., Valley, J.W., and Hamilton, M.A., 2004, Direct dating of Adirondack massif anorthosite by U-Pb SHRIMP analysis of igneous zircon: Implications for AMCG complexes: Geological Society of America Bulletin, v. 116, p. 1299–1317, doi: 10.1130/B25482.1.

McSween, H.Y., Abbott, R.N., and Raymond, L.A., 1989, Metamorphic conditions in the Ashe Metamorphic Suite, North Carolina Blue Ridge: Geology, v. 17, p. 1140–1143, doi: 10.1130/0091-7613(1989)017<1140:MCITAM>2.3.CO;2.

Merschat, C.E., and Cattanach, B.L., 2008, Bedrock geological map of the west half of the Asheville 1:100,000-scale quadrangle, North Carolina and Tennessee: North Carolina Geological Survey Geological Map Series 13.

Merschat, C.E., and Wiener, L.S., 1988, Geology of the Sandymush and Canton quadrangles, North Carolina: North Carolina Geological Survey Bulletin 90, scale 1:24,000.

Merschat, A.J., Hatcher, R.D., Jr., and Davis, T.L., 2005, The northern Inner Piedmont, southern Appalachians, USA: Kinematics of transpression and SW-directed mid-crustal flow: Journal of Structural Geology, v. 27, p. 1252–1281, doi: 10.1016/j.jsg.2004.08.005.

Merschat, C.E., Cattanach, B.L., Carter, M.W., and Wiener, L.S., 2006, Geology of the Mesoproterozoic basement and younger cover rocks in the west half of the Asheville 100000 quadrangle, North Carolina and Tennessee—An updated look, *in* Labotka, T.C., and Hatcher, R.D., Jr., eds., Field trip guidebook, 2006 Geological Society of America Southeastern Section meeting: Knoxville, Tennessee, University of Tennessee, p. 1–36.

Miller, B.V., Fetter, A.H., and Stewart, K.G., 2006, Plutonism in three orogenic pulses, Eastern Blue Ridge Province, southern Appalachians: Geological Society of America Bulletin, v. 118, p. 171–184, doi: 10.1130/B25580.1.

Miller, B.V., Stewart, K.G., and Whitney, D.L., 2010, Three tectonothermal pulses recorded in eclogite and amphibolite of the eastern Blue Ridge, southern Appalachians, *in* Tollo, R.P., et al., eds., From Rodinia to Pangea: The lithotectonic record of the Appalachian region: Geological Society of America Memoir 206, p. 701–724, doi: 10.1130/2010.1206(27).

Miller, C.F., Hatcher, R.D., Jr., Ayers, J.C., Coath, C.D., and Harrison, T.M., 2000, Age and zircon inheritance of Eastern Blue Ridge plutons, southwestern North Carolina and northeastern Georgia, with implications for magma history and evolution of the southern Appalachian orogen: American Journal of Science, v. 300, p. 142–172, doi: 10.2475/ajs.300.2.142.

Moecher, D.P., and Samson, S.D., 2006, Differential zircon fertility of source terranes and natural bias in the detrital zircon record: Implications for sedimentary provenance analysis: Earth and Planetary Science Letters, v. 247, p. 252–266, doi: 10.1016/j.epsl.2006.04.035.

Moecher, D.P., Samson, S.D., and Miller, C.F., 2004a, Precise time and conditions of peak Taconian granulite facies metamorphism in the southern Appalachian orogen, U.S.A., with implications for zircon behavior during crustal melting events: Journal of Geology, v. 112, p. 289–304, doi: 10.1086/382760.

Moecher, D.P., Tracy, R.J., and Miller, B.V., 2004b, Taconian metamorphism alive and well in the southern Blue Ridge: Geological Society of America Abstracts with Programs, v. 36, no. 2, p. 135.

Moecher, D.P., Massey, M.A., and Tracy, R.J., 2005, Timing and pattern of metamorphism in the Western and Central Blue Ridge, TN and NC: Status and outstanding problems, *in* Hatcher, R.D., Jr., and Merschat, A.J., eds., Blue Ridge geology geotraverse east of the Great Smoky Mountains National Park, western North Carolina: Carolina Geological Society Annual Field Trip Guidebook 2005, p. 57–66.

Moecher, D.P., Anderson, E.D., Clemons, K.M., and Massey, M.A., 2007, The pattern of tectonic overprinting in the western-central Blue Ridge by deformation propagating from the eastern Blue Ridge–Inner Piedmont convergence: Geological Society of America Abstracts with Programs, v. 39, no. 2, p. 79.

Montel, J.-M., Foret, S., Veschambre, M., Nicollet, C., and Provost, A., 1996, Electron microprobe dating of

monazite: Chemical Geology, v. 131, p. 37–53, doi: 10.1016/0009-2541(96)00024-1.

Odom, A.L., and Fullagar, P.D., 1973, Geochronologic and tectonic relationships between the Inner Piedmont, Brevard Zone, and Blue Ridge belts, North Carolina: American Journal of Science, v. 273-A, p. 133–149.

Odom, A.L., and Fullagar, P.D., 1984, Rb-Sr whole-rock and inherited zircon ages of the plutonic suite of the Crossnore complex, southern Appalachians, and their implications regarding the time of opening of the Iapetus ocean, *in* Bartholomew, M.J., ed., The Grenville event in the Appalachians and related topics: Geological Society of America Special Paper 194, p. 255–261.

Ownby, S.E., Miller, C.F., Berquist, P.J., Carrigan, C.W., and Fullagar, P.D., 2004, Geochemistry and U-Pb geochronology of a portion of the Mars Hill terrane, North Carolina–Tennessee: Constraints on origin, history, and tectonic assembly, *in* Tollo, R.P., et al., eds., Proterozoic tectonic evolution of the Grenville orogen in North America: Geological Society of America Memoir 197, p. 609–63, doi: 2 10.1130/0-8137-1197-5.609.

Parrish, R.R., 1990, U-Pb dating of monazite and its application to geological problems: Canadian Journal of Earth Sciences, v. 27, p. 1431–1450.

Patchett, P.J., and Samson, S.D., 2004, Ages and growth of the continental crust from radiogenic isotopes, *in* Rudnick, R., et al., eds., The crust: Elsevier, Treatise on Geochemistry 3, p. 321–348.

Pyle, J.M., and Spear, F.S., 2003, Four generations of accessory-phase growth in low-pressure migmatites from SW New Hampshire: American Mineralogist, v. 88, p. 338–351.

Pyle, J.M., Spear, F.S., Wark, D.A., Storm, L.C., and Daniel, C.G., 2005, Contributions to precision and accuracy of monazite microprobe ages: American Mineralogist, v. 90, p. 547–577, doi: 10.2138/am.2005.1340.

Rankin, D.W., 1975, The continental margin of eastern North America in the southern Appalachians: The opening and closing of the proto-Atlantic ocean: American Journal of Science, v. 275-A, p. 298–336.

Rankin, D.W., Espenshade, G.H., and Shaw, K.W., 1973, Stratigraphy and structure of the metamorphic belt in northwestern North Carolina and southwestern Virginia: A study from the Blue Ridge across the Brevard fault zone to the Sauratown Mountains anticlinorium: American Journal of Science, v. 273-A, p. 1–40.

Rankin, D.W., Drake, A.A., Jr., and Ratcliffe, N.M., 1990, Geologic map of the U.S. Appalachians showing the Laurentian margin and the Taconic orogen, *in* Hatcher, R.D., Jr., Thomas, W.A., and Viele, G.W., eds., The Appalachian-Ouachita Orogen in the United States: Boulder, Colorado, Geological Society of America, The Geology of North America, v. F-2.

Reed, J.C., and Bryant, B., 1964, Evidence for strike-slip faulting along the Brevard zone in North Carolina: Geological Society of America Bulletin, v. 75, p. 1177–1196, doi: 10.1130/0016-7606(1964)75[1177:EFSFAT]2.0.CO;2.

Rubatto, D., 2002, Zircon trace element geochemistry: Partitioning with garnet and the link between U-Pb ages and metamorphism: Chemical Geology, v. 184, p. 123–138, doi: 10.1016/S0009-2541(01)00355-2.

Rubatto, D., Williams, I.S., and Buick, I.A., 2001, Zircon and monazite response to prograde metamorphism in the Reynolds Range, central Australia: Contributions to Mineralogy and Petrology, v. 140, p. 458–468, doi: 10.1007/PL00007673.

Sinha, A.K., and Glover, L., III, 1978, U/Pb systematics of zircons during dynamic metamorphism: Contributions to Mineralogy and Petrology, v. 66, p. 305–310, doi: 10.1007/BF00373414.

Smith, H.A., and Barreiro, B., 1990, Monazite U-Pb dating of staurolite grade metamorphism in pelitic schists: Contributions to Mineralogy and Petrology, v. 105, p. 602–615, doi: 10.1007/BF00302498.

Spear, F.S., and Pyle, J.M., 2002, Apatite, monazite, and xenotime in metamorphic rocks, *in* Kohn, M.J., et al., eds., Phosphates: Geochemical, geobiological, and materials importance: Reviews in Mineralogy, v. 48, p. 293–335.

Su, Q., Goldberg, S.A., and Fullager, P.D., 1994, Precise U-Pb zircon ages of Neoproterozoic plutons in the southern Appalachian Blue Ridge and their implications for the initial rifting of Laurentia: Precambrian Research, v. 68, p. 81–95, doi: 10.1016/0301-9268(94)90066-3.

Tollo, R.P., Aleinikoff, J.N., Bartholomew, M.J., and Rankin, D.W., 2004, Neoproterozoic A-type granitoids of the central and southern Appalachians: Intraplate magmatism associated with episodic rifting of the Rodinian supercontinent: Precambrian Research, v. 128, p. 3–38, doi: 10.1016/j.precamres.2003.08.007.

Vauchez, A., 1987, Brevard fault zone, southern Appalachians: A medium-angle, dextral, Alleghanian shear zone: Geology, v. 15, p. 669–672, doi: 10.1130/0091-7613(1987)15<669:BFZSAA>2.0.CO;2.

Vavra, G., Schmid, R., and Gebauer, D., 1999, Internal morphology, habit and U-Th-Pb microanalysis of amphibolite-to-granulite facies zircons: Geochronology of the Ivrea Zone (Southern Alps): Contributions to Mineralogy and Petrology, v. 134, p. 380–404, doi: 10.1007/s004100050492.

Vinson, S.B., Miller, C.F., Fullagar, P.D., Hatcher, R.D., and Coath, C., 1999, Constraints on timing of Inner Piedmont plutonism, NC-SC, from ion microprobe U-Pb zircon analysis: Geological Society of America Abstracts with Programs, v. 31, no. 3, p. A30.

Willard, R.A., and Adams, M.G., 1994, Newly discovered eclogite in the southern Appalachian orogen, northwestern North Carolina: Earth and Planetary Science Letters, v. 123, p. 61–70, doi: 10.1016/0012-821X(94)90257-7.

Williams, M.L., and Jercinovic, M.J., 2002, Microprobe monazite geochronology: putting absolute time into microstructural analysis: Journal of Structural Geology, v. 24, p. 1013–1028, doi: 10.1016/S0191-8141(01)00088-8.

Williams, M.L., Jercinovic, M.J., and Terry, M.P., 1999, Age mapping and dating of mozanite on the electronic microprobe: Deconvoluting multistage tectonic histories: Geology, v. 27, p. 1023–1026.

Williams, M.L., Jercinovic, M.J., Goncalves, P., and Mahan, K., 2006, Format and philosophy for collecting, compiling, and reporting microprobe monazite ages: Chemical Geology, v. 225, p. 1–15, doi: 10.1016/j.chemgeo.2005.07.024.

Williams, M.L., Jercinovic, M.J., and Hetherington, C.J., 2007, Microprobe monazite geochronology: Understanding geologic processes by integrating composition and chronology: Annual Review of Earth and Planetary Sciences, v. 35, p. 137–175, doi: 10.1146/annurev.earth.35.031306.140228.

Wing, B.A., Ferry, J.M., and Harrison, T.M., 2003, Prograde destruction and formation of monazite and allanite during contact and regional metamorphism of pelites: Petrology and chronology: Contributions to Mineralogy and Petrology, v. 145, p. 228–250, doi: 10.1007/s00410-003-0446-1.

Manuscript Received 20 May 2010
Revised Manuscript Received 26 October 2010
Manuscript Accepted 26 October 2010